

Analysis of Block Shear Failure

Analýza porušení vytržením skupiny šroubů

MASTER'S THESIS

Study Programme: Civil Engineering

Study Branch: Building Structures

Supervisor: prof. Ing. František Wald, CSc.

Bc. David Sekal

Munich, 2019



ZADÁNÍ DIPLOMOVÉ PRÁCE

I. OSOBNÍ A STUDIJNÍ ÚDAJE

Příjmení: Sekal Jméno: David Osobní číslo: 426319
Zadávající katedra: Ocelových a dřevěných konstrukcí
Studijní program: Stavební inženýrství
Studijní obor: Konstrukce pozemních staveb

II. ÚDAJE K DIPLOMOVÉ PRÁCI

Název diplomové práce: Analýza porušení vytržením skupiny šroubů
Název diplomové práce anglicky: Analysis of Block Shear Failure

Pokyny pro vypracování:

Shrnutí literatury, cíle práce, experimenty z literatury, návrhově orientovaný FEA model, analytický model, validace modelů, verifikace modelů, shrnutí, další cíle v oblasti

Seznam doporučené literatury:

Topkaya C. A finite element parametric study on block shear failure of steel tension members, Journal of Constructional Steel Research, 2004

prEN 1993-1-8, Eurocode 3: Design of steel structures, Part 1.8: Design of joints" Brussels, 2018

EN 1993-1-8, Eurocode 3: Design of steel structures, Part 1.8: Design of joints, Brussels, 2005

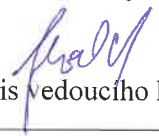
Jméno vedoucího diplomové práce: prof. Ing. František Wald, CSc.

Datum zadání diplomové práce: 1.10.2018

Termín odevzdání diplomové práce: 6.1.2019

Údaj uveďte v souladu s datem v časovém plánu příslušného ak. roku


Podpis vedoucího práce


Podpis vedoucího katedry

III. PŘEVZETÍ ZADÁNÍ

Beru na vědomí, že jsem povinen vypracovat diplomovou práci samostatně, bez cizí pomoci, s výjimkou poskytnutých konzultací. Seznam použité literatury, jiných pramenů a jmen konzultantů je nutné uvést v diplomové práci a při citování postupovat v souladu s metodickou příručkou ČVUT „Jak psát vysokoškolské závěrečné práce“ a metodickým pokynem ČVUT „O dodržování etických principů při přípravě vysokoškolských závěrečných prací“.

1.10.2018

Datum převzetí zadání


Podpis studenta(ky)

Declaration

I hereby declare that this assignment is my own work and is not copied from any other person's work and that I stated all the information resources used in conformity with Methodical guide for ethical development of university final thesis.

In Munich, 6.1.2019



Acknowledgment

I would like to express my special thanks of gratitude to professor František Wald not only for his guidance, help and valuable advises but also for suggestion of this interesting topic.

I would also like to thank the Technical University of Munich, Chair of Metal Structures for providing me with access to their technical facilities and especially Ms. Nadine Maier for willing help.

Then, for the English language consulting and proofreading, my thanks go to Victor Kosinski.

Finally, I would like to thank my family and friends for supporting me during my studies and sharing with me successes as well as failures.

Abstract

The work is focused on the analysis of a block shear failure mode of bolted connections. The first part includes general description of the block shear failure mechanism, literature review and summary of current possible design approaches.

In second part, the experiments from literature are presented and in accordance to them, research oriented finite element models are validated. Then follows a verification of component based finite element models with the validated research-oriented model and analytical models. Verification includes sensitivity study of pitch distance, plate thickness and size of eccentricity.

In the last part, the benchmark example of a tension bracing member connection is presented and compared with results of chosen analytical models.

Keywords

Block shear, block tearing, shear, tension, bolted connection, yield stress, engineering stress, true stress, engineering strain, true strain, rupture, validation, verification

Abstrakt

Práce je zaměřena na analýzu módu porušení vytržením skupiny šroubů. První část práce obsahuje základní popis módu porušení, shrnutí literatury zabývající se tímto tématem a výčet současných možných návrhových přístupů.

V druhé části jsou pak popsány experimenty získané z literatury a dle nich je vytvořen a validován pokročilý konečně prvkový model. Dále jsou na těchto pokročilých modelech a různých analytických modelech verifikovány návrhové modely využívající metodu konečných prvků založenou na metodě komponent. Verifikace zahrnuje studii citlivosti jejíž proměnné parametry jsou rozteče šroubů, tloušťka plechu a velikost excentricity.

V poslední části je pak představen ověřovací příklad přípoje ztužidla a porovnán s výsledky vybraných analytických modelů.

Klíčová slova

Vytržení skupiny šroubů, smyk, tah, šroubový přípoj, mez kluzu, inženýrské napětí, reálné napětí, inženýrské přetvoření, reálné přetvoření, přetržení, validace, verifikace

Table of Contents

1	Introduction.....	- 6 -
2	State of art	- 7 -
2.1	Phenomenon.....	- 7 -
2.2	Literature review	- 8 -
2.3	Analytical models from design standards	- 13 -
2.3.1	EN 1993-1-8: 2005 - Design of joints	- 13 -
2.3.2	AISC 360-10 – Specification for Structural Steel Buildings.....	- 14 -
2.3.3	EN 1993-1-8: 2020 - Design of joints	- 15 -
2.3.4	CSA-S16-09 – Design of steel structures	- 16 -
2.4	Finite element analysis.....	- 17 -
2.4.1	General principles of meshing.....	- 18 -
2.5	Component based finite element method.....	- 20 -
2.6	Experiments.....	- 21 -
2.6.1	Geometries	- 22 -
2.6.2	Materials	- 23 -
3	Objective of the thesis.....	- 24 -
4	Research oriented finite element analysis.....	- 25 -
4.1	Model geometry	- 25 -
4.2	Loading	- 26 -
4.3	Mesh study	- 27 -
4.4	Validation.....	- 32 -
4.4.1	Compared parameters	- 32 -
4.4.2	Validation results	- 33 -
5	Design oriented finite element analysis.....	- 36 -
5.1	Concetric connections	- 36 -
5.1.1	Verification	- 37 -
5.1.2	Sensitivity study.....	- 46 -

5.2	Eccentric connection	- 52 -
5.2.1	Geometry	- 52 -
5.2.2	Materials	- 52 -
5.2.3	Verification	- 53 -
5.2.4	Sensitivity study.....	- 54 -
6	Benchmark case	- 57 -
6.1	Benchmark case specification.....	- 57 -
6.1.1	Geometry	- 57 -
6.1.2	Materials	- 58 -
6.2	Analytical models.....	- 58 -
6.2.1	EN 1993-1-8: 2005	- 58 -
6.2.2	EN 1993-1-8: 2020	- 59 -
6.3	Component based finite element method.....	- 59 -
6.3.1	Results.....	- 59 -
6.4	Comparison of models	- 60 -
7	Conclusion	- 62 -
7.1	Validation.....	- 62 -
7.2	Verification	- 62 -
7.3	Future work	- 64 -
	References.....	- 65 -
	List of tables	- 66 -
	List of figures.....	- 67 -

1 INTRODUCTION

The thesis is focused on the design of bolted connections which tend to be sensitive to block shear failure. There are several possible approaches of steel connections design.

The most common way of designing against block shear failure is using the analytical models, which are described in codes. The major advantage of these models is, that they can be used in most cases and they are the easy to apply. In this work, the comparison of analytical models will include currently valid 1st generation of Eurocode, US structural steel design code A360-10, 2nd generation of Eurocode which is planned to be issued after 2020, Canadian structural steel design standard CSA S16-09 and analytical models proposed by (Driver et al., 2005) and (Topkaya et al., 2004)

In theory, another possible design approach is the component method. In principle, the steel joint is divided into various components – column web, bolts, welds etc. Then, according to the design rules described in Eurocode, a determination of strength, stiffness and deformation capacity of each component follows. Finally, to get the overall joint behaviour, the components are reassembled. However, the form of usage of the component method for design against block shear failure has not been described yet.

With the development of computational technology, it is possible to create accurate finite element models. These can be validated on experiments; therefore, the behaviour of numerical simulation is close to the physical test. Their main advantage is, that once the appropriate finite element model is created, it is possible to carry the parametric study on it by minor modifications without performing additional physical tests. However, making an accurate finite element model is laborious and, due to many variables, such as definition of boundary conditions, meshing etc., the results are not always representative. Complex finite element models of joints are commonly used in the field of science but exceptionally in the structural engineering design practise.

The approach which employs the last two mentioned methods is called component based finite element method (CBFEM). As apparent, it combines aspects of finite element method and component method to provide the satisfactory way of designing steel joints, while simultaneously getting them to comply with valid standards. In contrary to the complex finite element simulations, it is commonly used for designing of steel joints in practise.

2 STATE OF ART

2.1 PHENOMENON

Bolted connections of steel structures are designed to withstand several modes of failure. The mode with a lowest bearing capacity determines the failure.

The block shear failure occurs in cases of not optimal design due to the structural geometry. It is the potential failure mode for gusset plates, fin plates, coped beams, single or double angles and tee connections, where significant tension / shear forces are present, as there is not enough space to comply with recommended pitches and end distances of bolts. Simply put, the block of material ruptures from the connecting element, gusset plate, web, angle leg etc., without a pronounced violation of bolts.

The block shear failure develops in most cases by yielding along the shear planes and rupture on the tensile plane in a first mode. In the second mode, yielding along the tension plane and a rupture along the shear plane may occur, but these cases are quite rare, due to smaller ductility of steel in tension compared to the ductility in shear (shear modulus of steel $G = 77000$ MPa, Young's modulus $E = 200000$ MPa). Block tearing is present in bolted connections usually because of the reduced section area, but it can also be found in welded joints. This work is focused on the bolted connections only.

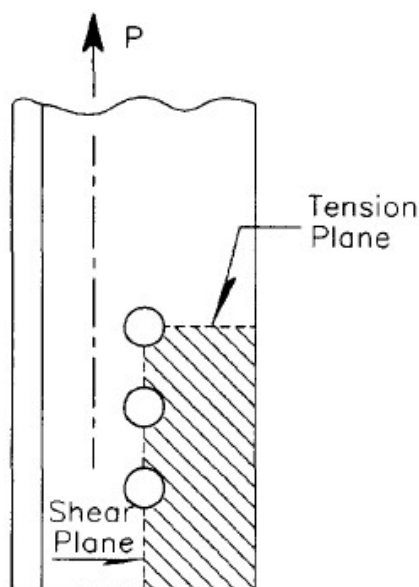


Figure 2.1 - Typical block shear failure mechanism (Cunningham T. J., Orbison J. G., Ziemian R. D., 1994)

2.2 LITERATURE REVIEW

Whitmore R.E. - *Experimental Investigation of Stresses in Gusset Plates*, 1952

R.E. Whitmore invented so-called Whitmore method. The method describes how a force from a brace spreads through a gusset plate. The basis of the method is Whitmore section – an effective width in tension, which can be found on a line connecting the beginning of the joint, 30° to each side in the connecting element along the line of force, to the end of the joint (last row of bolts). In figure 2.2 it is marked as l_w . The actual stress can be obtained as:

$$\sigma = \frac{F}{(l_w \cdot t)} \quad (1)$$

where t represents gusset plate thickness and F is an acting force.

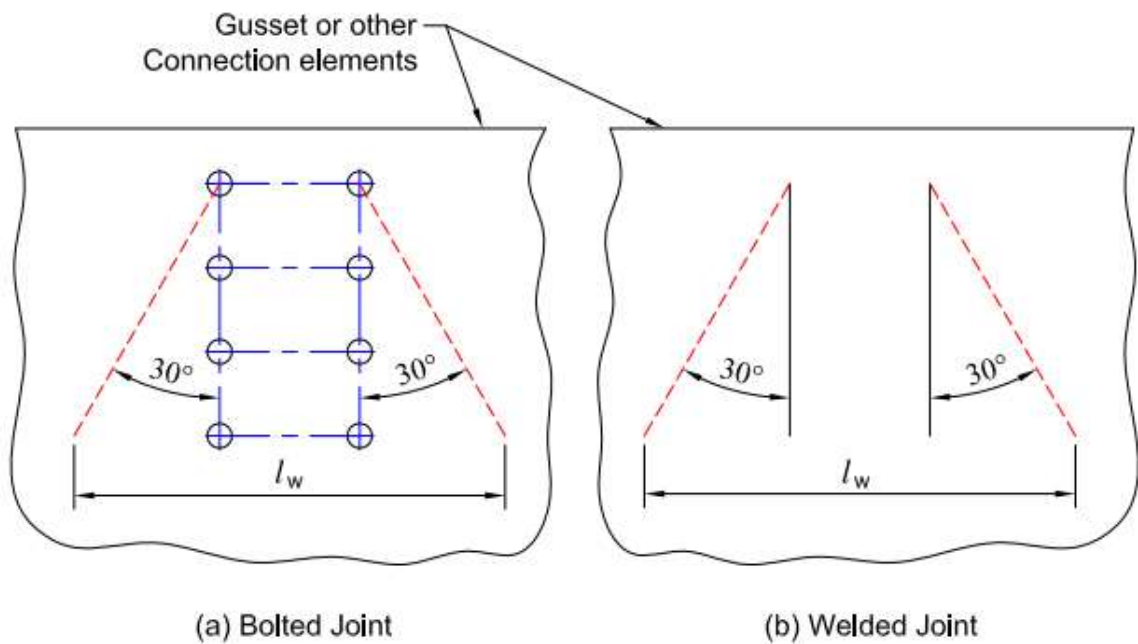


Figure 2.2 - The Whitmore section (Thornton W. A., Lini C., 2011)

Kulak G. L., Grondin G. Y. - *Block Shear Failure in Steel Members — A Review of Design Practice*, 2001

The authors compared analytical models in different national standards (European, American, Canadian, Australian and Japanese) with gathered experimental results. They also separated the results into categories according to the connection type – gusset plate, coped beam, single angles and tees, double angles and determined the safety ratio as: analytical model resistance / test results. Finally, they suggested their own analytical equations:

$$\text{For angles and gusset plates it is } P_u = A_{nt} \cdot \sigma_u + 0,6 \cdot \sigma_y \cdot A_{gv} \quad (2)$$

$$\text{and for coped beam webs it is } P_u = 0,5 \cdot A_{nt} \cdot \sigma_u + 0,6 \cdot \sigma_y \cdot A_{gv} \quad (3)$$

where P_u is block tearing resistance [N]

A_{nt} is net area subjected to tension [mm²]

A_{gv} is gross area subjected to shear [mm²]

σ_u is ultimate stress [MPa]

σ_y is yield stress [MPa]

Topkaya C. A. - *Finite Element Parametric Study on Block Shear Failure of Steel Tension Members*, 2004

Topkaya used previously carried experiments and made a parametric finite element models in accordance with them. Thanks to these models, he found out, among other things, that the stress on a shear plane is lower than the tension yield stress but higher than a shear stress - $0,6F_y$. The so-called effective shear stress is given as a function of the connection length. He claims, that the effective shear stress decreases as the connection length increases, see Fig. 2.3.

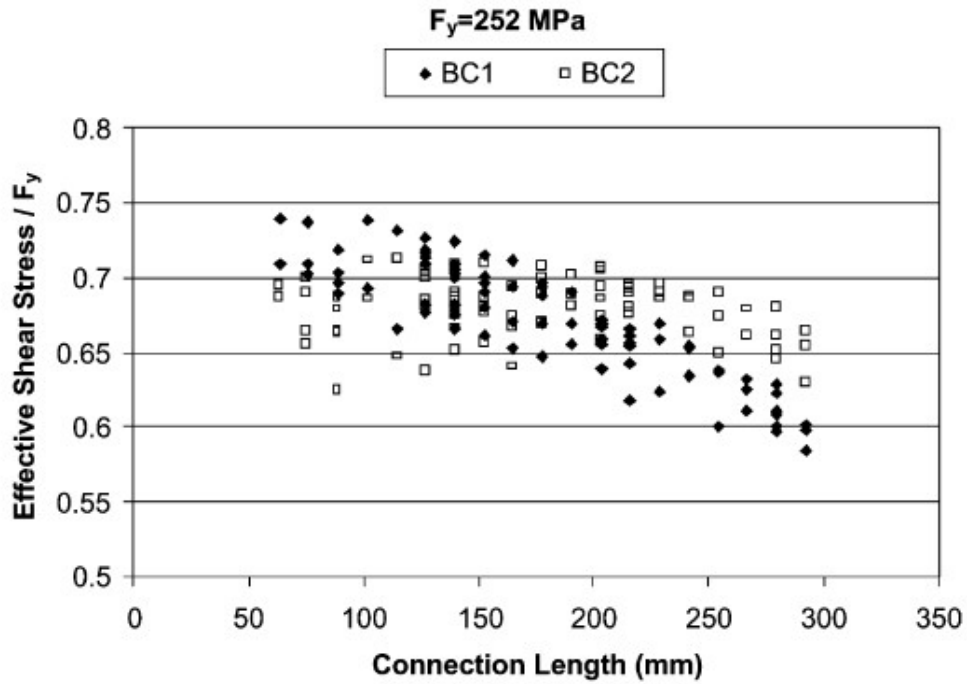


Figure 2.3 - Effect of boundary conditions on effective stress (Topkaya C. A., 2004)

This fact led him to conclusion, that a single value – $0,6 F_y$ could not be used in cases where more accurate predictions are needed.

Author also examined the effect of in-plane or out-of-plane eccentricity. Topkaya says, that the in-plane eccentricity decreases the resistance up to 15 % and is mostly influenced by the connection length. He also mentioned that for the connection length up to 150 mm, there is no reduction of capacity needed. In case of out of plane eccentricity, the difference between the connections without eccentricity was at most 5 %. Due to these findings he concluded that the block shear capacity stays unaffected by out-of-plane eccentricity.

In the end, he suggested three possible block shear capacity equations:

$$R_n = \left(0,25 + 0,35 \frac{F_u}{F_y} - \frac{Cl}{2800} \right) F_y A_{gv} + F_u A_{nt} \quad (4)$$

where R_n is block tearing resistance [N]

F_u is ultimate stress [MPa]

F_y is yield stress [MPa]

Cl is connection length [mm]

A_{gv} is gross area subjected to shear [mm²]

A_{nt} is net area subjected to tension [mm²]

simplified equation if the effective shear stress is based only on the ultimate-to-yield ratio is

$$R_n = \left(0,20 + 0,35 \frac{F_u}{F_y}\right) F_y A_{gv} + F_u A_{nt} \quad (5)$$

and finally, when the average value for effective shear stress is taken

$$R_n = 0,48 F_u A_{gv} + F_u A_{nt} \quad (6)$$

All these equations are developed for the concentric loading. In case of eccentric, long connections he suggests decreasing the load bearing capacity by 10 %.

Driver R. G., Grondin G. Y., Kulak G. L. - *Unified block shear equation for achieving consistent reliability*, 2005

The authors collected a database of block shear experiments including gusset plates, angles, tees and coped beams tests. They came up with the equation, which changes factors depending on the type of connection:

$$P_u = R_t A_{nt} F_u + R_v A_{gv} \left(\frac{F_y + F_u}{2\sqrt{3}} \right) \quad (7)$$

where P_u is block tearing resistance [N]

R_t, R_v are equivalent stress factors for unified equation [—]

A_{nt} is net area subjected to tension [mm²]

A_{gv} is gross area subjected to shear [mm²]

F_u is ultimate stress [MPa]

F_y is yield stress [MPa]

Equivalent stress factors vary from 0,3 - 1 according to the type of connection. The advantage of the formula is, that it gives, according to the authors, more realistic results than the codes do and that it is uniform for both eccentric and concentric connections.

However, there are additional factors introduced which goes against the idea of making the analytical models comprehensible and transparent.

Jönsson J. – *Block Failure in Connections Including Effects of Eccentric Loads*, 2014

The main objective of that publication is to reconsider the influence of eccentric loading on block shear failure mode. Jönsson believes, that the correct approach is to create simple interaction formulas related to the other ones used in codes for cross section analysis - the interaction of normal force, shear force and bending moment. In the end there would be a simple equation:

$$\left(\frac{N}{N_R} + \frac{M}{M_R}\right)^2 + \left(\frac{V}{V_R}\right)^2 \leq 1 \quad (8)$$

where N , M , V are actual section forces and N_R , M_R , V_R are individual resistances of the joint.

The question here is whether is it still problem of block tearing because, as it was mentioned before, this failure mode is typical for bracing tension members (concentric in most cases), or members with very small eccentricity – gusset plates, coped beams, angles – where, as observed in Topkaya's study [1], the eccentricity plays a small role (up to 15 %). On the other hand, it needs to be agreed, that, for atypical connections with large eccentricity, there should be an instrument which allows us to calculate the resistance.

2.3 ANALYTICAL MODELS FROM DESIGN STANDARDS

2.3.1 EN 1993-1-8: 2005 - DESIGN OF JOINTS

The rules presented in Eurocode are separated into two categories – “symmetric group of bolts subjected to concentric loading” and “group of bolts subjected to eccentric loading”.

Concentric loading

For concentric loading the design block tearing resistance $V_{eff,1,Rd}$ is given by:

$$V_{eff,1,Rd} = \frac{f_u A_{nt}}{\gamma_{M2}} + \left(\frac{1}{\sqrt{3}} \right) f_y A_{nv} / \gamma_{M0} \quad (9)$$

where A_{nt} is net area subjected to tension [mm²]

A_{nv} is net area subjected to shear [mm²]

γ_{M0} is material design factor which equals to 1 [–]

γ_{M2} is material design factor which equals to 1,25 [–]

f_u is ultimate strength [MPa]

f_y is yield strength [MPa]

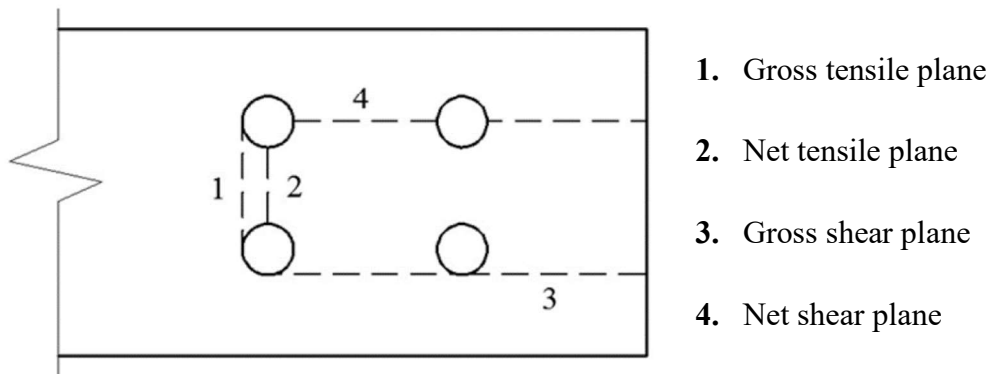


Figure 2.4 – Failure planes (Teh L. H., Clements D. D. A., 2012)

Equation given in (9) does not respect the idea mentioned before, that block shear failure appears in two possible modes. There is either the rupture on a net tension plane together with yielding on a gross shear plane or the rupture on a net shear plane together with net tension

plane rupture. The formula given in (9) takes the conservative values from these two modes combined.

An interesting fact is, that in the previous Eurocode; *Eurocode 3: Design of Steel Structures, ENV 1993-1-1, Brussels, 1992*, a A_{gv} – gross sectional shear area was used, and as pointed out by Geoffrey L. Kulak and Gilbert Y. Grondin in *Block Shear Failure in Steel Members – A Review of Design Practice: “The rules presented in Eurocode are based on the fundamental assumption that this mode of failure consists of tensile rupture along the line of fastener holes on the tension face of the hole group accompanied by gross section yielding in shear at the row of fastener holes along the shear face of the hole group.”*. On the top of this, according to other authors, in previous Eurocode, contrary to the Eurocode in use today, the results for analytical models were very close to the experimental results.

Eccentric loading

For eccentric loading the design block tearing resistance $V_{eff,2,Rd}$ is given by:

$$V_{eff,2,Rd} = 0,5 \cdot \frac{f_u A_{nt}}{\gamma_{M2}} + \left(\frac{1}{\sqrt{3}}\right) f_y A_{nv} / \gamma_{M0} \quad (10)$$

The 0,5 ratio represents non-uniform stress distribution due to eccentric loading. Even though it seems to be in most cases conservative solution and it doesn't consider the actual size of eccentricity.

2.3.2 AISC 360-10 – SPECIFICATION FOR STRUCTURAL STEEL BUILDINGS

The approach of American Institute of Steel Construction is less conservative than the current valid Eurocode's formulas because it uses the ultimate strength for the shear resistance part. Nevertheless, the capacity is limited by the right side of the equation, which corresponds with the idea, that when the yield stress is reached on the gross shear plane, the rupture appears on the tension plane. The factor U_{bs} reduces the tension plane resistance due to a non-uniform stress distribution in a same way as Eurocode does.

$$R_n = 0,6F_u A_{nv} + U_{bs} F_u A_{nt} \leq 0,6F_y A_{gv} + U_{bs} F_u A_{nt} \quad (11)$$

where R_n is block tearing resistance [N]

A_{gv} is gross area subjected to shear [mm²]

A_{nv} is net area subjected to shear [mm²]

A_{nt} is net area subjected to tension [mm²]

F_u is ultimate strength [MPa]

F_y is yield strength [MPa]

U_{bs} is 1 or 0,5 [-]

The load resistance safety factor for LRFD method is $\phi = 0,75$ [-]

It is worth to mention that Australian Standard, AS 4100-1998 - Steel structures, which could also be included in analytical models' comparison, uses the identic equation as the AISC 360-10.

2.3.3 EN 1993-1-8: 2020 - DESIGN OF JOINTS

The Eurocode that will be issued after 2020 has significantly changed its approach compared to the current code. The equations are still separated into two groups with the respect to the position of an acting force.

Concentric loading

$$V_{eff,1,Rd} = \left[A_{nt}f_u + \min\left(\frac{A_{gv}f_y}{\sqrt{3}}; \frac{A_{nv}f_u}{\sqrt{3}}\right) \right] / \gamma_{M2} \quad (12)$$

Variables are described in previous paragraphs.

In contrast to current Eurocode, (12) considers the gross shear plane instead of the net shear plane which, according to (Kulak and Grondin, 2005), corresponds better with the experiment results. It also implements an idea similar to AISC that there are two possible ways of block shear failure – either a rupture along the net shear plane followed by a rupture on a net tension plane occurs (when the connection is short and wide), or the net tension rupture appears before the ultimate stress on a shear plane fully develops (in case of long and narrow connections).

Eccentric loading

$$V_{eff,2,Rd} = \left[0,5A_{nt}f_u + \min\left(\frac{A_{gv}f_y}{\sqrt{3}}; \frac{A_{nv}f_u}{\sqrt{3}}\right) \right] / \gamma_{M2} \quad (13)$$

Ratio 0,5 represents non-uniform stress distribution on a tension plane due to eccentric loading.

2.3.4 CSA-S16-09 – DESIGN OF STEEL STRUCTURES

Canadian steel structures standard equation is based on findings of (Driver et al., 2005):

$$R_n = F_u A_{nt} + 0,3 \cdot (F_y + F_u) \cdot A_{gv} \quad (14)$$

Variables are described in previous paragraphs.

After separation of $\sqrt{3} \approx 0,6$, which comes from von-Mises yield criterion, (14) can be rewritten as:

$$R_n = F_u A_{nt} + 0,6 \cdot 0,5 \cdot (F_y + F_u) \cdot A_{gv} \quad (15)$$

From this adjusted equation it is apparent that authors used mean value between ultimate stress and yield stress which represents the contribution of strain hardening to the shear resistance capacity.

2.4 FINITE ELEMENT ANALYSIS

The development of finite element analysis (FEA) in a field of structural engineering began in 1940 and its usage is closely linked with the improvement of digital computational technology.

FEA is, according to (Daryl L. Logan, 2010): Numerical method which is used in situations where we can't obtain the solution with linear or differential equations. It is handful in cases with complicated geometries, material properties and loadings. Typically, the unknowns for structural problems are the displacements and stresses.

In the process of modelling, the complex shape is divided into equivalent smaller, simpler interconnected units – called finite elements. Consequently, instead of solving the problem for the entire body, equations are created for each finite element and, in order to obtain the global solution; they are combined into a stiffness matrix. Finally, instead of one complex differential function there is a large number of simple, e.g. linear or cubic, equations which are convenient for computer to solve. Whereas the differential equations have a finite solution, the solution of FEA is an approximation, nevertheless the approximation so accurate that it is sufficient for engineering purposes. The actual accuracy depends on the number of elements created – generally speaking, the denser the mesh of elements is, the more accurate solution is obtained.

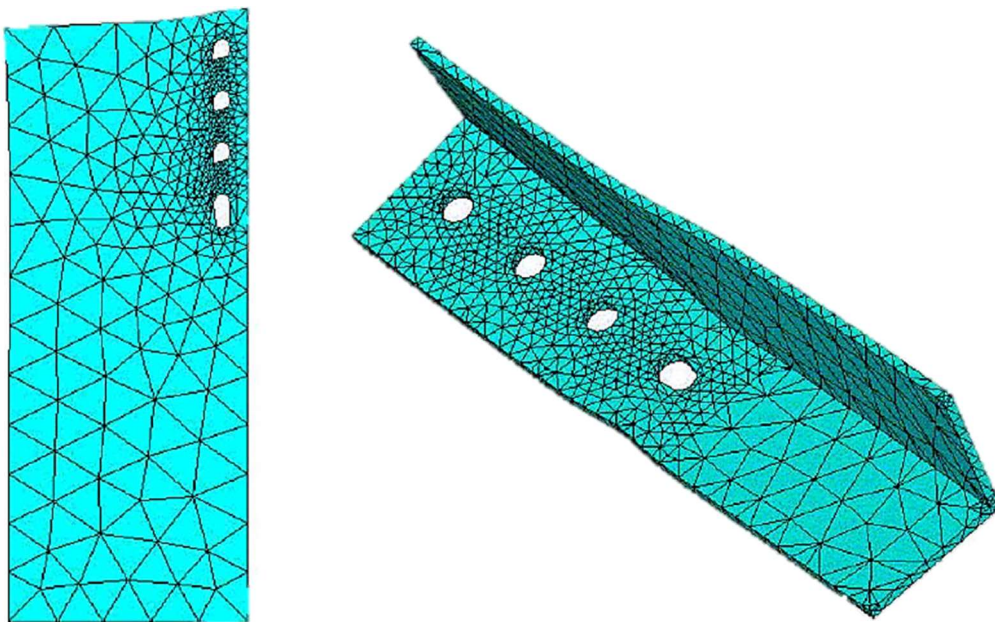


Figure 2.5 - Research oriented finite element models (Topkaya C. A., 2004)

According to the (Daryl Logan, 2010) the steps carried in finite element analysis are following:

- 1) Discretization and selection of element type
- 2) Selection of displacement function
- 3) Definition of the strain versus displacement and stress versus strain relationships
- 4) Creation of element stiffness matrix
- 5) Incorporation of boundary conditions
- 6) Solving of equations
- 7) Evaluation of results

In FEA softwares such as ANSYS, the mentioned steps can be adjusted, but most of them is carried by the software automatically.

2.4.1 GENERAL PRINCIPLES OF MESHING

Meshing is a process of dividing the component into finite number of elements. Aim of it is to create a mesh dense enough to distribute the acting load uniformly without expressive step changes. However, the denser the mesh is, the more elements there are, and the more computational effort is needed. Therefore, it is desired to find balance between these two requirements. Optimal solution is creating a dense mesh in places where are:

- 1) Changes in geometry
- 2) Contacts between components
- 3) Close to restraints
- 4) In areas where are high gradients expected

Not only the mesh density but also the shape of element and classification of grid affect the accuracy and efficiency of the solution.

As the model in this work is three-dimensional, there are according to [14] several basic element shapes which can be used:

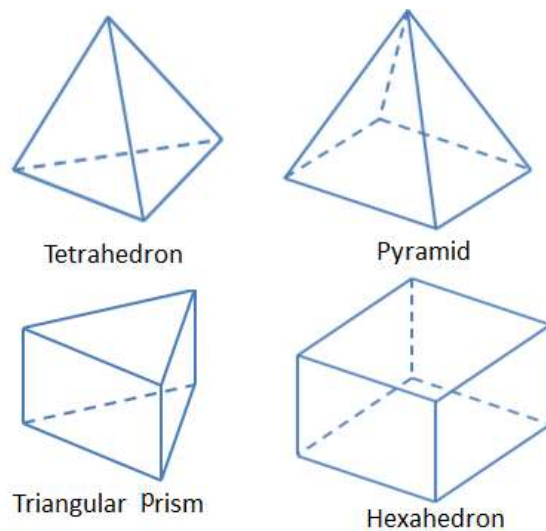


Figure 2.6 - Basic three-dimensional element shapes

From those, the hexahedron (also called hex or brick) achieves, generally said, the highest accuracy of solution with the same number of elements.

Another thing which affects the solution is the classification of a grid. On the one hand, there are structured grids, which have regular pattern and converge faster with a higher accuracy, on the other hand, there are unstructured grids with irregular pattern which are less effective. The mixture of those two types is called hybrid grid.

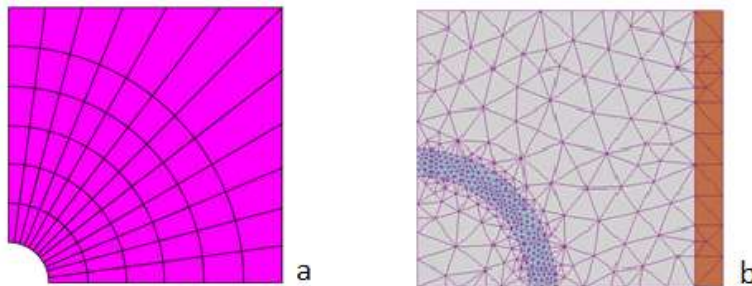


Figure 2.7 - Grid classifications – a) structured grid b) unstructured grid

Signs of a good mesh are:

1. High rate of convergence – good mesh converges faster which means that the final solution is achieved faster
2. Absence or minimum elements with sharp angles or short edges

2.5 COMPONENT BASED FINITE ELEMENT METHOD

Component based finite element method (CBFEM) combines both – component method and finite element analysis. It uses the experimental and analytical findings on which is based component method together with finite element analysis. Normally laborious component method is, with the use of computer and proper software support, a good tool for detailed design of steel joints in practice.

It works on a basis, that fasteners – bolts, welds but also bolt holes, contacts etc. are replaced by components which have pre-defined mechanical behaviour and plates are formed of shell elements which are suitable for finite element analysis.

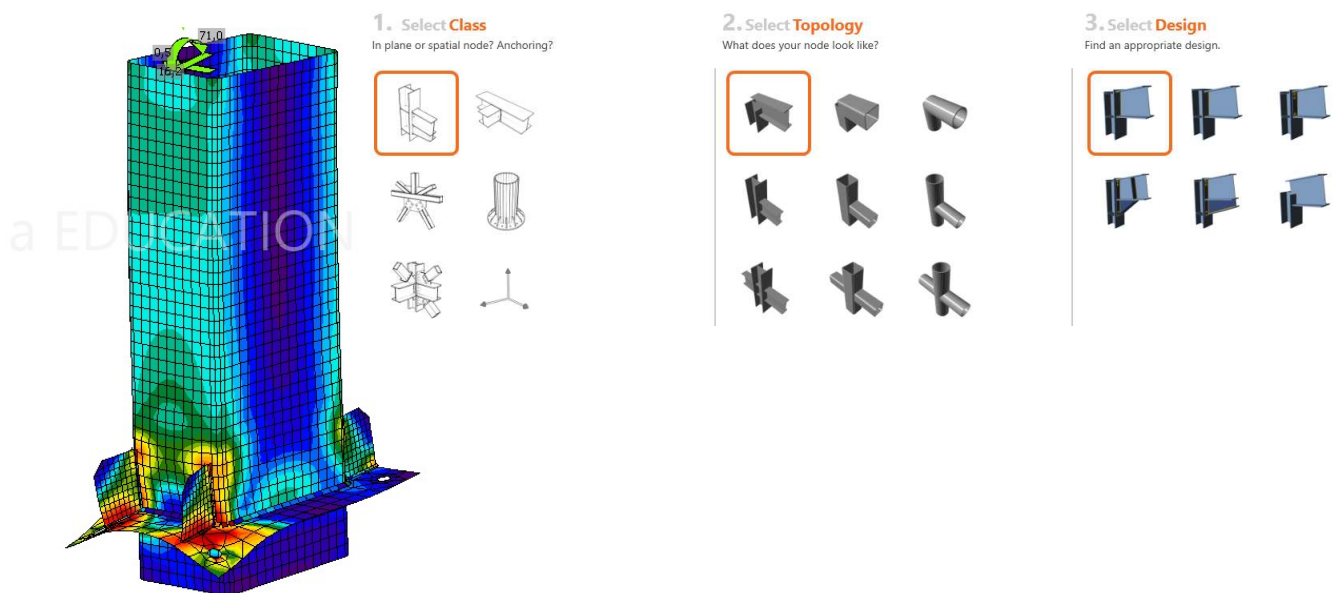


Figure 2.8- Illustrative example of interface and graphical results in IDEA StatiCa 9 – software which employs CBFEM

2.6 EXPERIMENTS

The experiments used in this work for validation were carried and described by Huns B. B. S., Grondin G., Driver R. G. [15].

Huns, Grondin and Driver tested two configurations of gusset plate bolted connections – a long and narrow connection and a short and wide connection – in order to propose new analytical model for calculating a block shear failure mode.

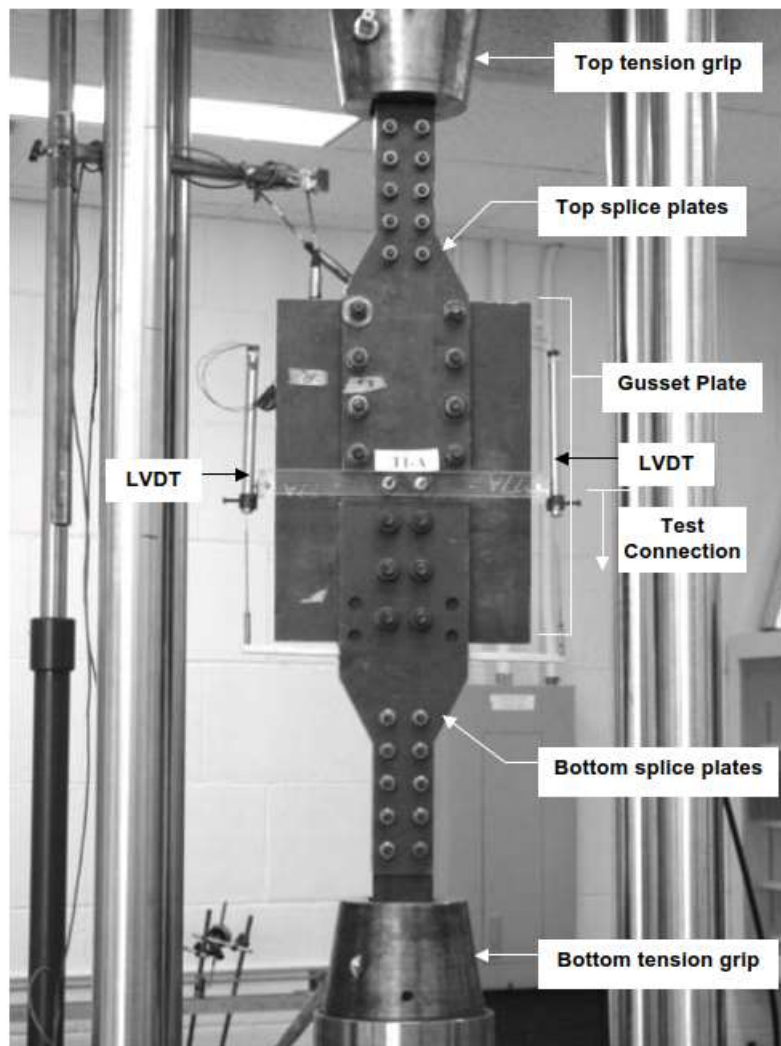


Figure 2.9 - Test set-up (Huns B. B. S., Grondin G., Driver R. G., 2002)

2.6.1 GEOMETRIES

The geometries of tested specimens can be seen in figures 2.10 and 2.11. The tested gusset plates are 6,6 mm thick, the bolts used are $\frac{3}{4}$ inch (19,05 mm) and the bolt holes are match drilled so the bolts are in bearing from the beginning of test.

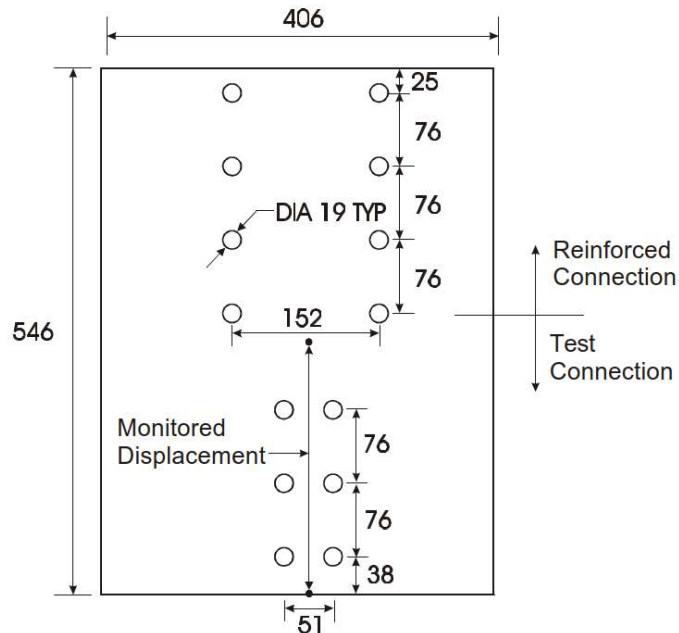


Figure 2.10 - Test specimen T1 (Huns B. B. S., Grondin G., Driver R. G., 2002)

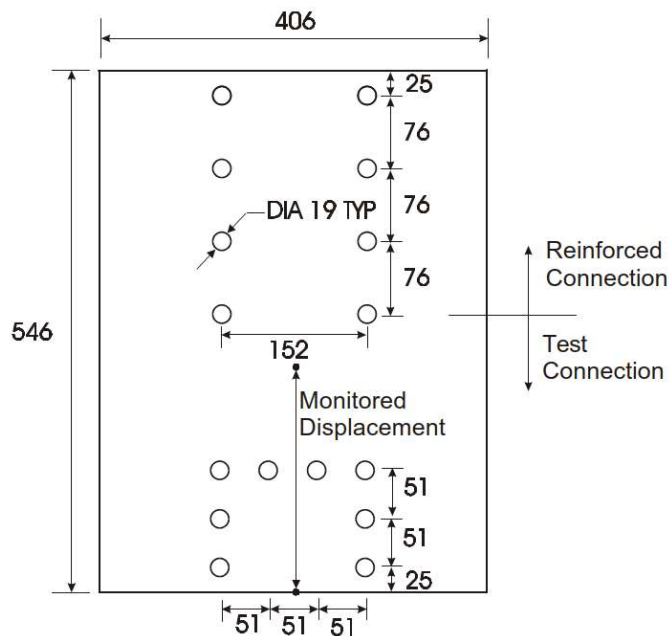


Figure 2.11 - Test specimen T2 (Huns B. B. S., Grondin G., Driver R. G., 2002)

2.6.2 MATERIALS

Since both specimens are made of the same steel sheet, mean values of F_y , F_u , ν and E apply for both. As for the description of plastic hardening a multilinear function is used. That curve was described by authors [15] and derived from the coupon tensions tests. The curve starts at a yield point, where the elastic part of the stress versus strain curve ends. Up to that point, there is a linear function that has a slope coefficient equal to E .

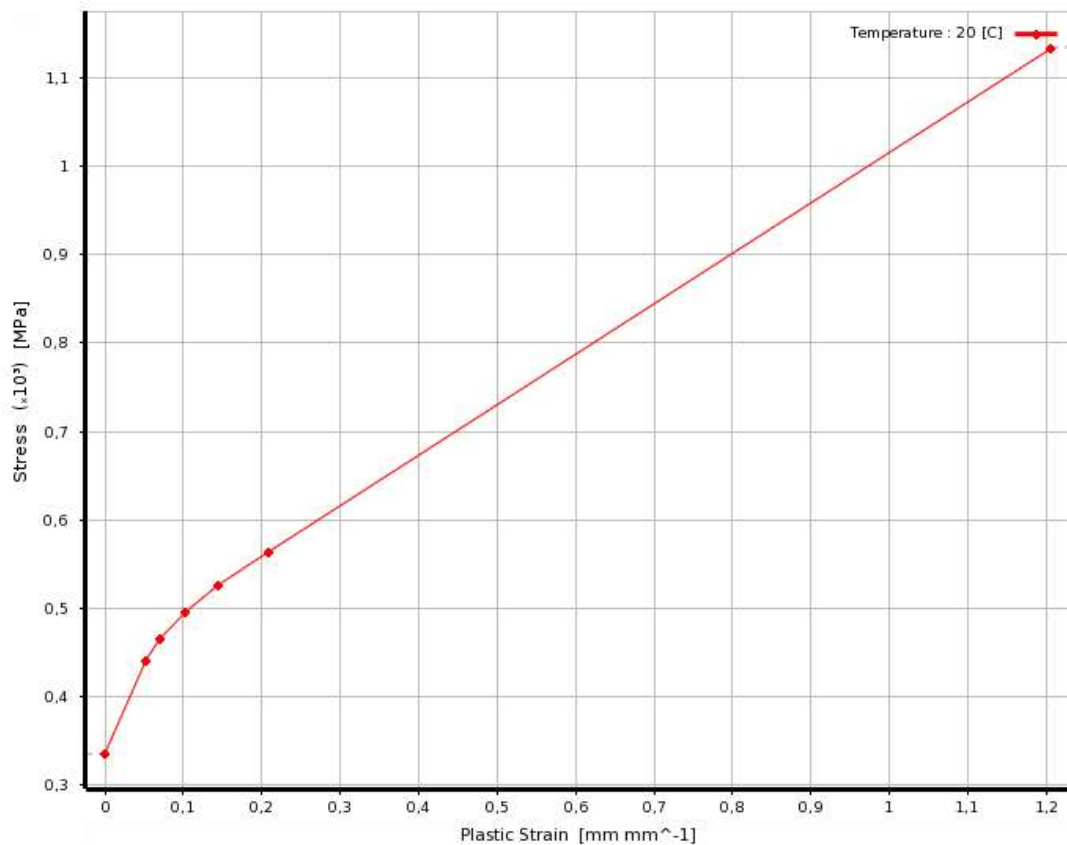


Figure 2.12 - Multilinear isotropic hardening, ANSYS interface

Plate properties:

Modulus of elasticity E [MPa]	Static yield stress F_y [MPa]	Static ultimate stress F_u [MPa]	Poisson's ratio ν [-]
197553	336	450	0,3

Bolts A325:

Modulus of elasticity E [MPa]	Static yield stress F_y [MPa]	Static ultimate stress F_u [MPa]
200000	660	830

3 OBJECTIVE OF THE THESIS

The aim of this work is to verify the design against block shear failure mode of steel bolted connections by Component based finite element method (CBFEM). Another goal is to compare the model from the upcoming EN 1993-1-8: 2020 with other national standards and analytical models from literature.

To achieve these, the main objective is divided into several parts:

1. Validation of two research oriented finite element models (ROFEA) with the experimental data obtained from literature
2. Verification of the CBFEM models with validated ROFEA and analytical models
3. Sensitivity study of CBFEM models containing plate thickness, pitch distance and size of eccentricity variable parameters
4. Provision of benchmark case which can be used and easily followed when designing against block shear failure mode

4 RESEARCH ORIENTED FINITE ELEMENT ANALYSIS

One of the motivations for creating a research-oriented model is the fact, that the validated numerical simulation can substitute some of the missing experimental data. In the original paper (Huns et al., 2002), there is not described stress vs. strain behaviour of the tested specimens, which is one of the observed parts in the verification process. On the contrary, there is a well-described creation of research oriented finite element model.

In this thesis, research oriented finite element analysis (ROFEA) is made using computational software ANSYS Workbench 18.0 which was developed to simulate various engineering problems with an aid of finite element analysis. In this case, it is the simulation of structural experiments described in previous chapters. On the one hand the demand is to create model and boundary conditions that are as close to the experiment as possible, whereas on the other hand it is desired to make the model effective and simple enough to reduce the computational effort needed. It is an iterative process that leads to the simplification of the model without losing the significance of its accuracy. As a source of information, the validation process described by (Huns et al., 2002) is used.

4.1 MODEL GEOMETRY

Since the deformation during the test was measured at the beginning and at the end of the connection, it is not necessary to model the whole experiment setup. The reduced model geometries can be seen in a Figure 4.1.

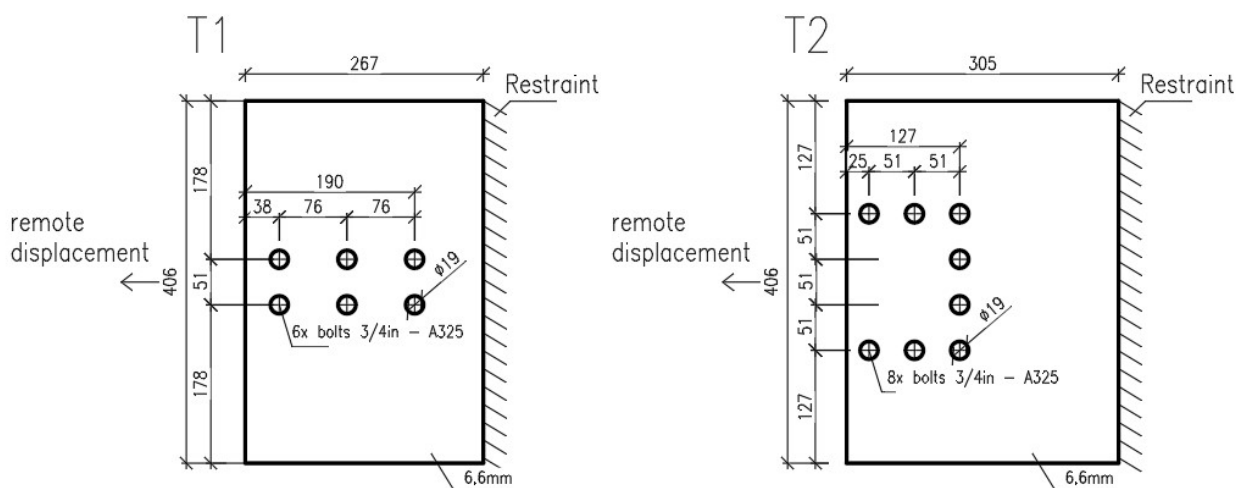


Figure 4.1 - Simplified geometries used for FEM simulations

4.2 LOADING

Due to the fact, that the splice plates are significantly thicker and therefore much more rigid than the inspected gusset plates it is assumed that all the bolts move together in a rigid frame defined by the initial pitches and gauge distances. The loading process was represented by a remote displacement that matches the test procedure.

A first idea was to include bolts in the model by using simple solids – three cylinders bound together and then realize the remote displacement on their shanks. However, the application of a remote displacement (six to eight solids), bolt contacts, and bolts themselves significantly influenced the computational effort needed.

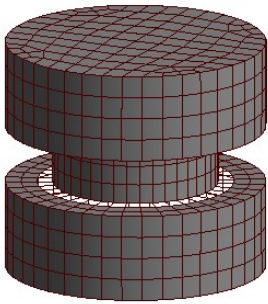


Figure 4.2 – Initial concept of bolts

Eventually, it became clear that the best solution would be to apply the remote displacement only on the nodes on half (since the bolts were match drilled) of each bolt hole in the chosen direction.

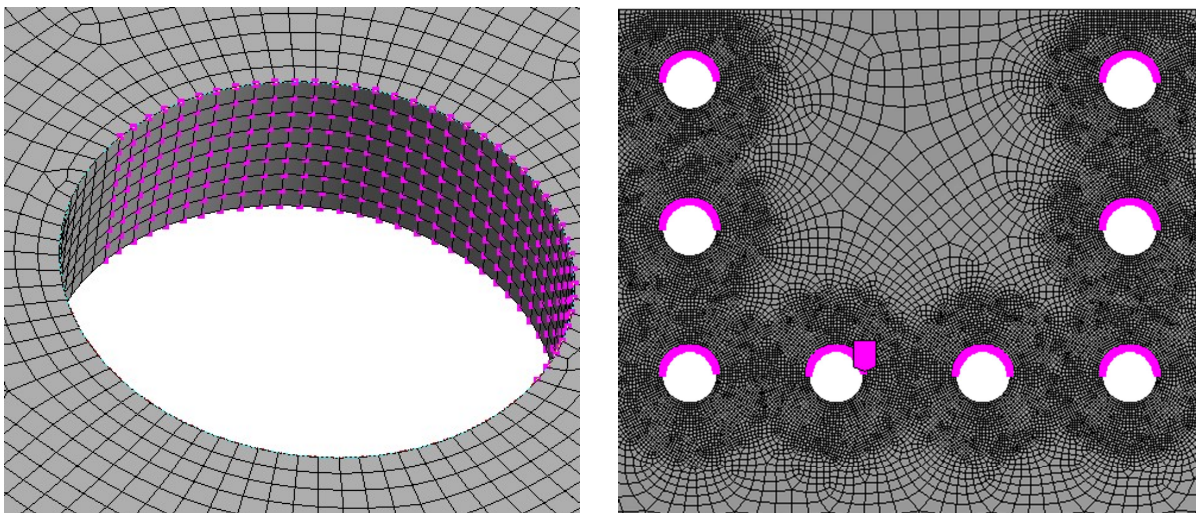


Figure 4.3 - Detail of a bolt hole and nodal selection

4.3 MESH STUDY

The purpose of mesh study is to observe the response of the model to different mesh methods. The tested parameters are the number and type of elements. Several mesh generations were carried, followed by comparisons with what is believed to be the most accurate mesh. Since the models are on the same basis, the mesh is optimised for one of them before using the same method for another.

Mesh 1 - Automatically generated mesh

The first compared mesh is automatically generated by the ANSYS software.

Number of the elements: 22621

Type of the element: Triangular prism

Computational time: 1,5 hours

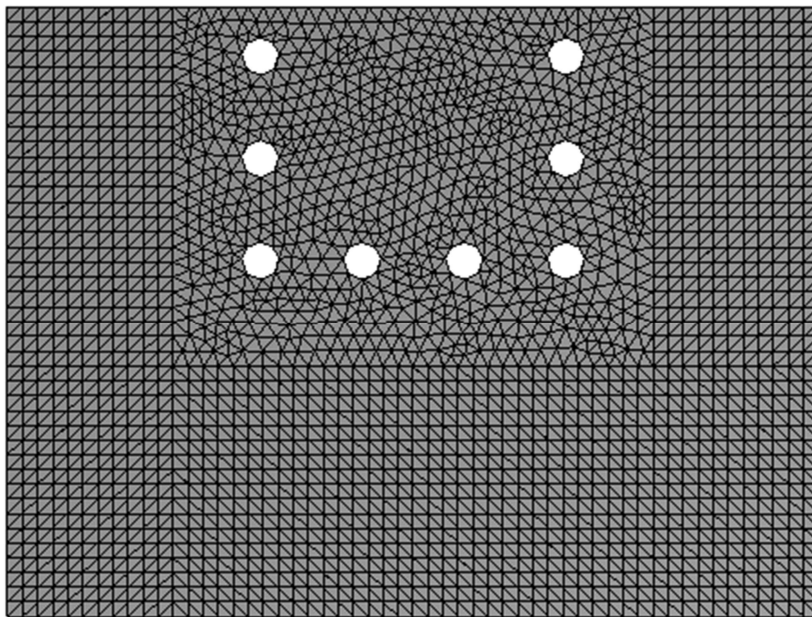


Figure 4.4 - Automatically generated mesh

1. Mesh 2 - Dense, automatically generated mesh

For the second solution an automatically generated, denser mesh is used.

Number of the elements: 58636

Type of the element: Triangular prism

Computational time: 4 hours

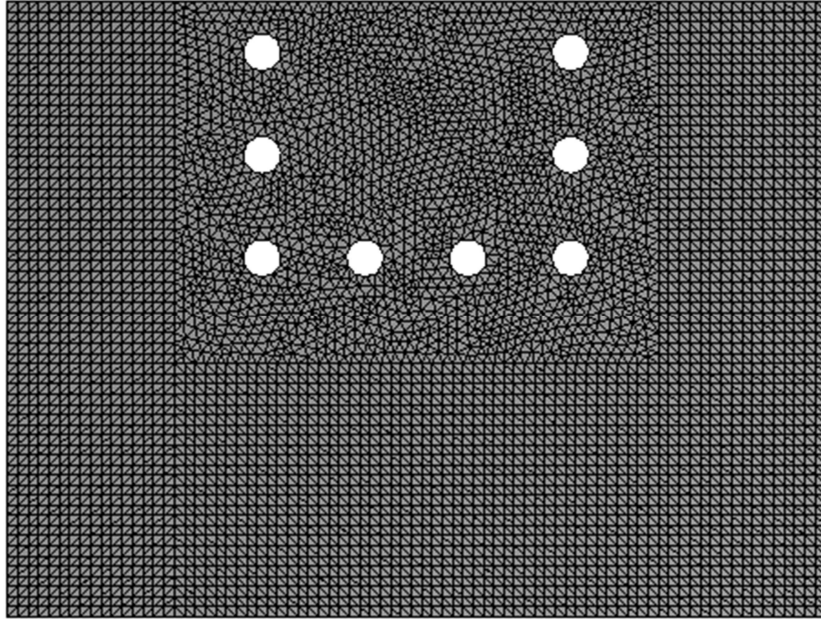


Figure 4.5 - Dense, automatically generated mesh

Mesh 3 - Hexahedron-dominant mesh

As it was mentioned before, in case of finite element method, generally speaking, the most effective element type is the hexahedron. Therefore, in this step, it was used in combination with a sparse mesh.

Number of the elements: 3258

Type of the element: Hexahedron

Computational time: 2 hours

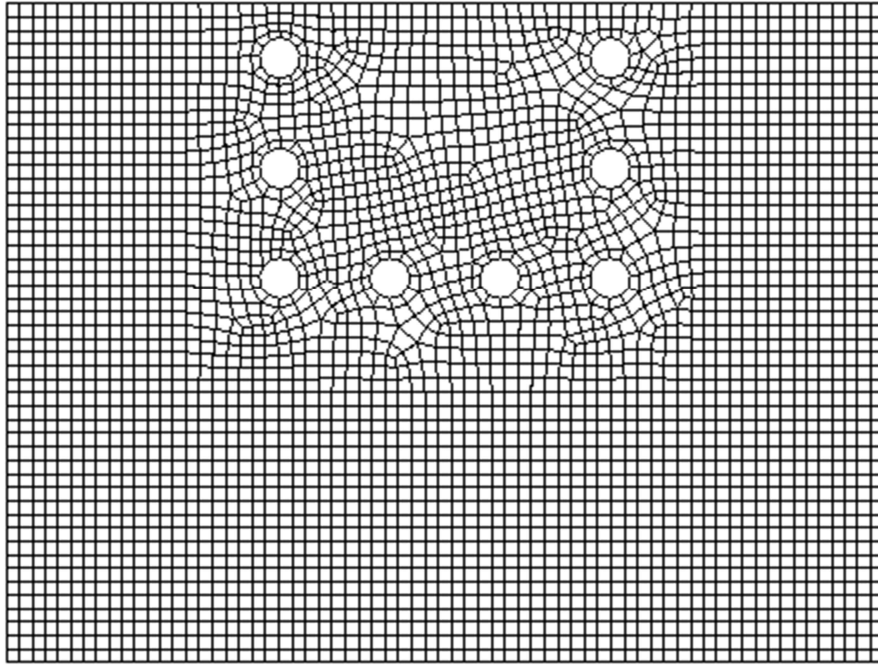


Figure 4.6 – Hexahedron-dominant mesh

Mesh 4 - Locally dense, hexahedron-dominant mesh

To save on computational time, the dense mesh is used only in areas where a high gradient is expected – locally, around the bolt holes with a radially structured grid. A hexahedron element type is used.

The long computational time may be acceptable in case of scientific purposes but as mentioned in previous chapters, is unsuitable for design practise where we need to solve problems in real time.

This mesh method is believed to be the most accurate, therefore other meshes are compared to it.

Number of the elements: 190264

Type of the element: Hexahedron

Computational time: 26 hours

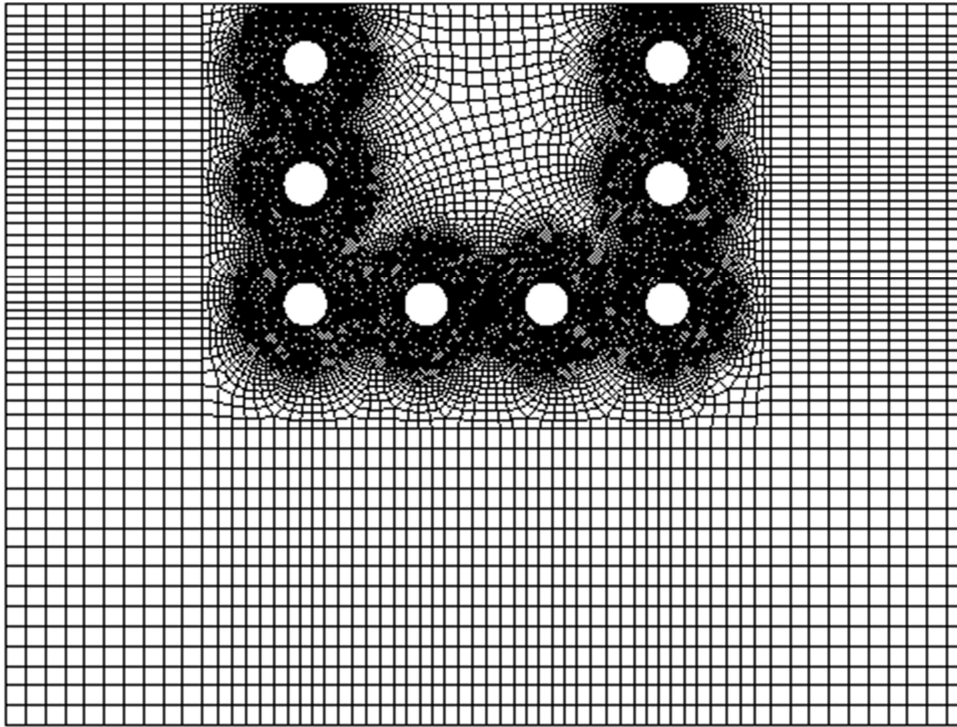


Figure 4.7 – Locally dense, hexahedron-dominant mesh

Mesh comparison

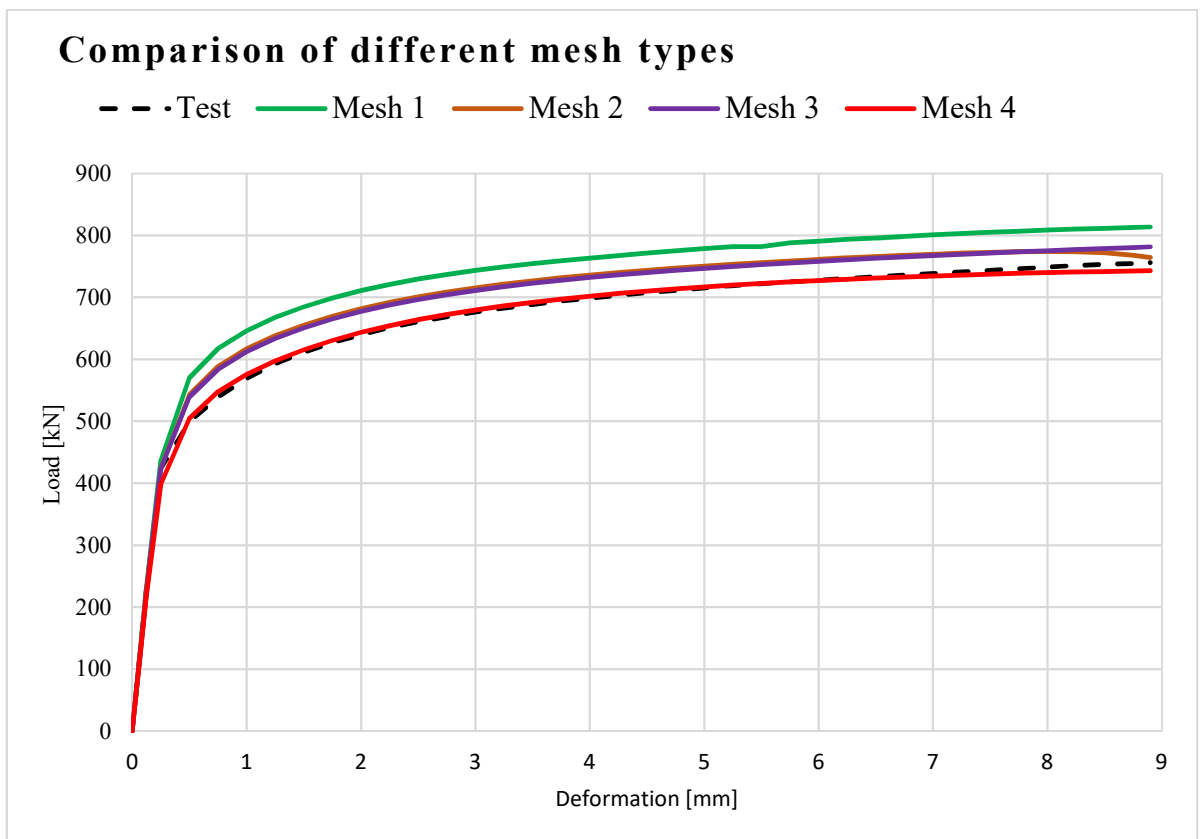


Figure 4.8 – Comparison of results of different mesh types

As a measure of compliance with the mesh 4 a standard deviation is used:

$$s = \sqrt{\frac{1}{N-1} \cdot \sum_{i=1}^N (x_i - x')^2} \quad (16)$$

where s is a standard deviation [kN]

N is a number of deformation steps [-]

x_i is a mesh's 1,2,3 result in specific step [kN]

x' mesh's 4 result in specific step [kN]

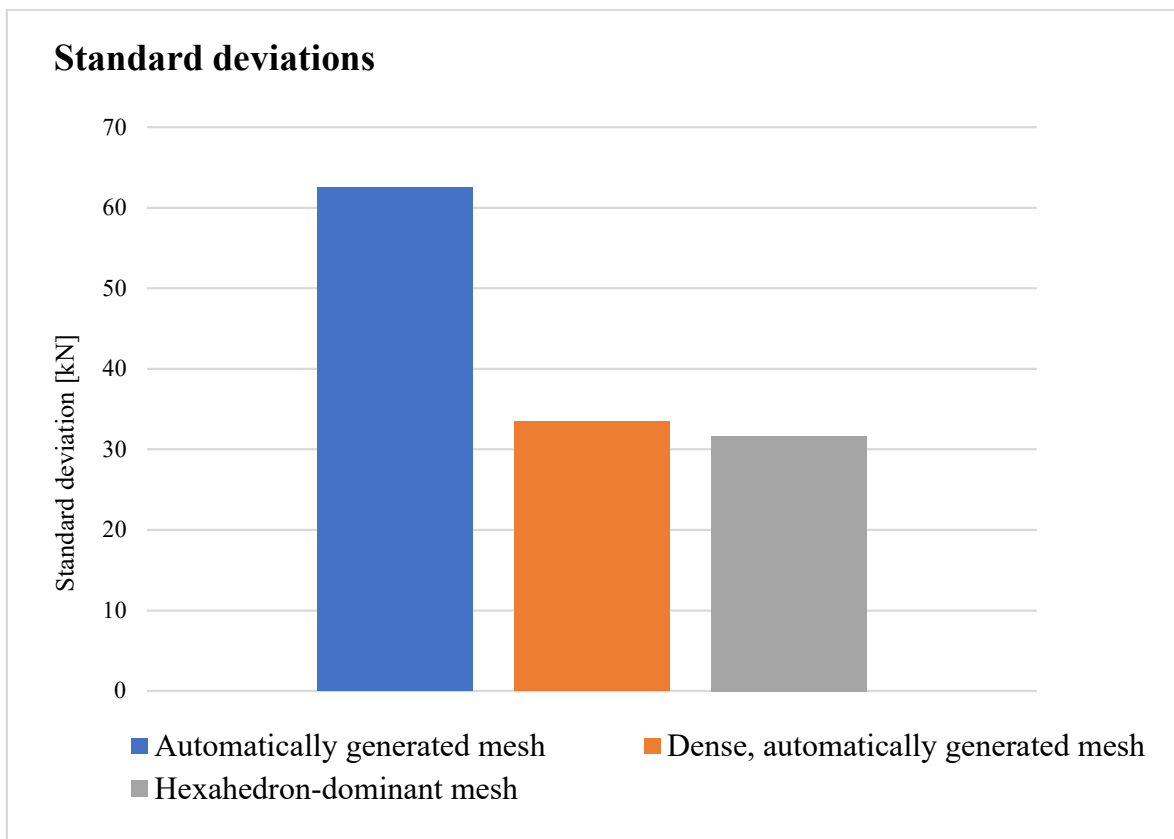


Figure 4.9 - Comparison of standard deviations

4.4 VALIDATION

According to (Wald et al, 2017), validation is a process where the numerical solution, in this case the ROFEA model, is compared with experimental data. It is a reverse procedure where we know the test results and we want to validate chosen parameters with a corresponding numerical solution.

The compared parameters are selected in accordance to the purpose of the computational model. The numerical solution does not necessarily need to correspond with the experimental parameters which are not important to the observed phenomenon.

Wald says, that the evaluation of validation and verification results depends, among other things, on the engineer's judgement, as there is no consensus on an acceptable rate of difference between the test and numerical results and even the rate may vary for each type of connection. However, recommended values are up to 5% on a side of safety in case of resistance and up to 20% on a side of safety in case of stiffness.

4.4.1 COMPARED PARAMETERS

1. **Failure mode**
2. **Initial stiffness - $N_{j,ini}$**
3. **Peak load - F_{peak}**
4. **Resistance at 2 mm deformation - F_{2mm}**
5. **Resistance at 5% strain - $F_{0,05}$**

Unfortunately, as the stress versus strain results are not part of the original paper from which the experimental data was derived, this parameter could not be compared in the validation process. Nevertheless, the true stress versus strain behaviour can be obtained from validated computational model and through it, it is possible to obtain engineering stress versus strain results. The process of obtaining those values is described in chapter 5.1.

6. **Serviceability limit state resistance at 2/3 of test ultimate deformation $F_{2/3}$**

4.4.2 VALIDATION RESULTS

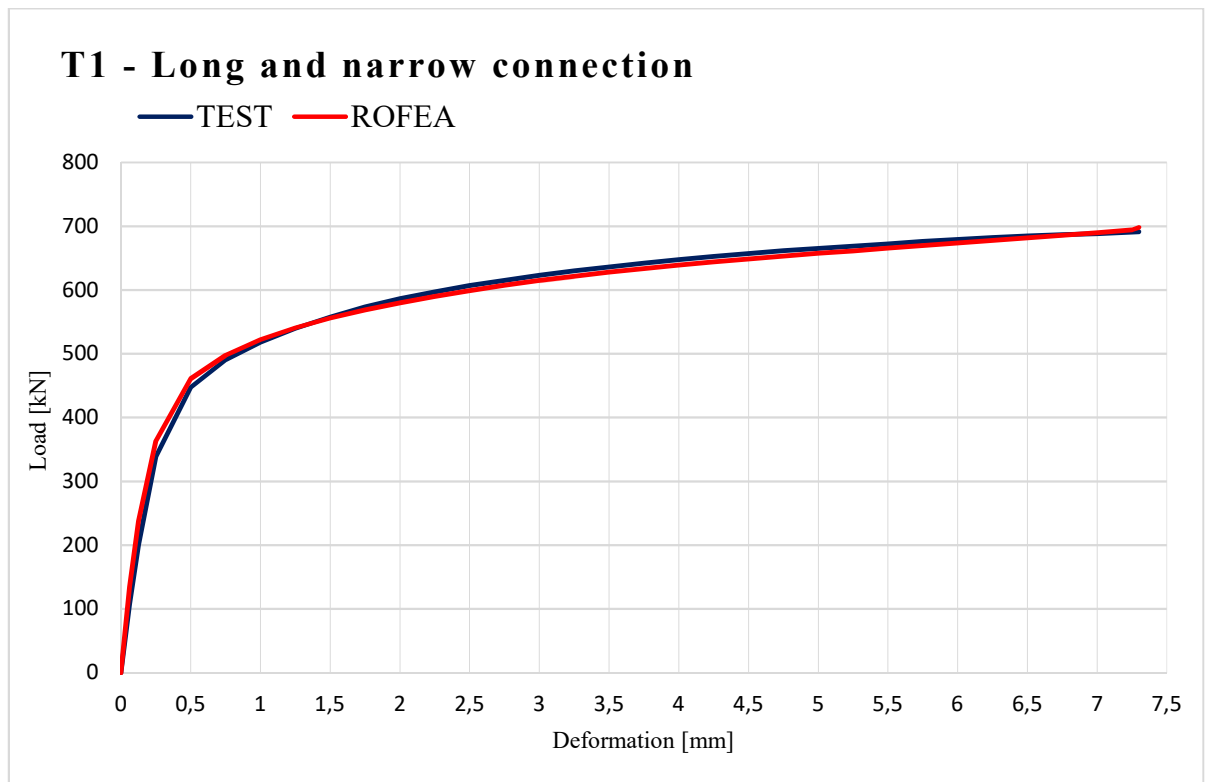


Figure 4.10 - Load versus deformation plot, ROFEA and experimental curves, T1

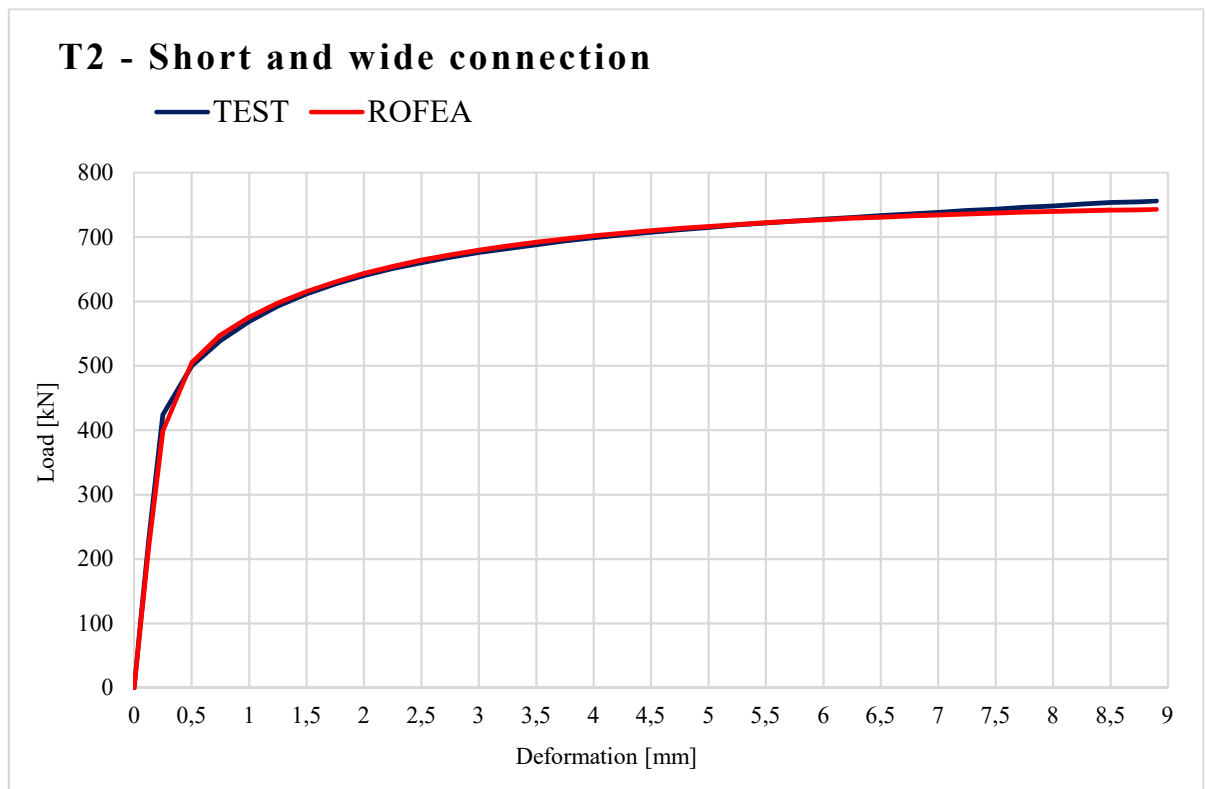


Figure 4.11 – Load versus deformation plot, ROFEA and experimental curves, T2

Table 4.1 – Results of validation, T1

T1 specimen	Values			Experiment/ROFEA ratio [-]
Compared parameters	Units	Experiment	ROFEA	
$N_{j,ini}$	[MN/m]	1717,7	2153,4	0,80
F_{peak}	[kN]	691,2	698,1	0,99
F_{2mm}	[kN]	586,2	580,1	1,01
$F_{0,05}$	[kN]	N/A	486,3	N/A
$F_{2/3}$	[kN]	663,0	654,5	1,01

Table 4.2 – Results of validation, T2

T2 specimen	Values			Experiment/ROFEA ratio [-]
Compared parameters	Units	Experiment	ROFEA	
$N_{j,ini}$	[MN/m]	1846,4	1773,1	1,04
F_{peak}	[kN]	756,0	742,9	1,02
F_{2mm}	[kN]	639,9	643,3	0,99
$F_{0,05}$	[kN]	N/A	421,0	N/A
$F_{2/3}$	[kN]	727,0	726,5	1,00

Despite some differences between numerical simulation and physical tests, there is a good rate of compliance in tested parameters. Maximal difference between the compared values is 20% in case of initial stiffness of T1 model. For initial stiffness, the higher rate of difference is acceptable because the value is dependent on factors like whether the bolts were really in bearing from the beginning of the physical test or whether the size of elements around bolt holes in case of ROFEA was appropriate. However, besides this one value, the other compared parameters vary between 0 – 4 % so the models can be used for the further CBFEM design-oriented model verification. Admittedly, some minor deviations are acceptable for engineering purposes.

Also, it is worth to note that on a deformed numerical model, signs typical for block shear failure mechanism could be observed, such as necking on a tension plane or yielding on the outer plane of bolt holes etc.

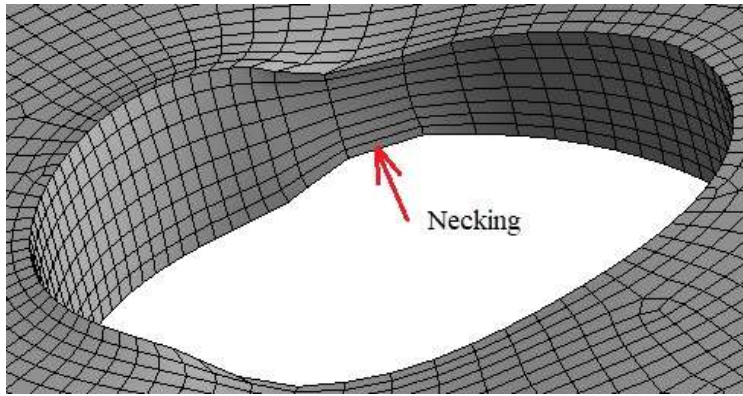


Figure 4.12 – *Deformed bolt hole, necking on a tension plane*

The good correspondence between numerical simulation and experiment is also thanks to the information and data obtained from the original paper [15], where authors carried validation themselves.

5 DESIGN ORIENTED FINITE ELEMENT ANALYSIS

Design oriented finite element analysis is done with the aid of CBFEM software IDEA StatiCa, version 9. This software combines the finite element method with the component method and offers an alternative to conventional analytical models and laborious component method. In contrary to ROFEA from chapter 4, IDEA software uses 2D shell elements for plates whereas fasteners (welds, bolts, contacts etc.) are represented by components with pre-defined properties based on experimental findings.

5.1 CONCENTRIC CONNECTIONS

Two CBFEM models with geometries and materials corresponding to physical tests described in chapter 2.6 were created.

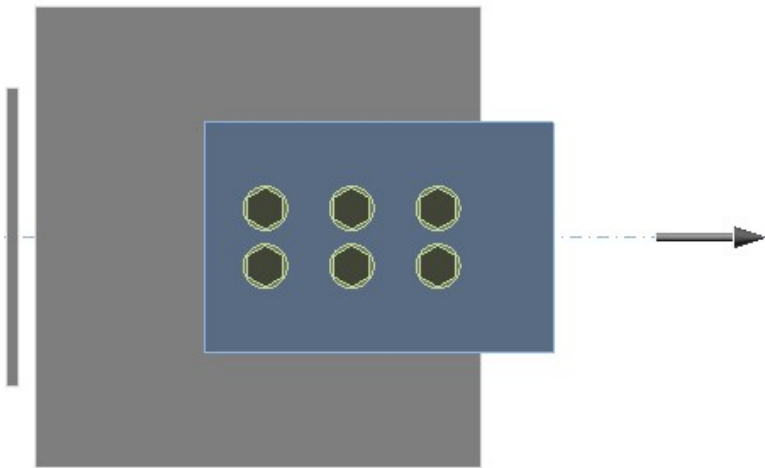


Figure 5.1 - CBFEM model T1

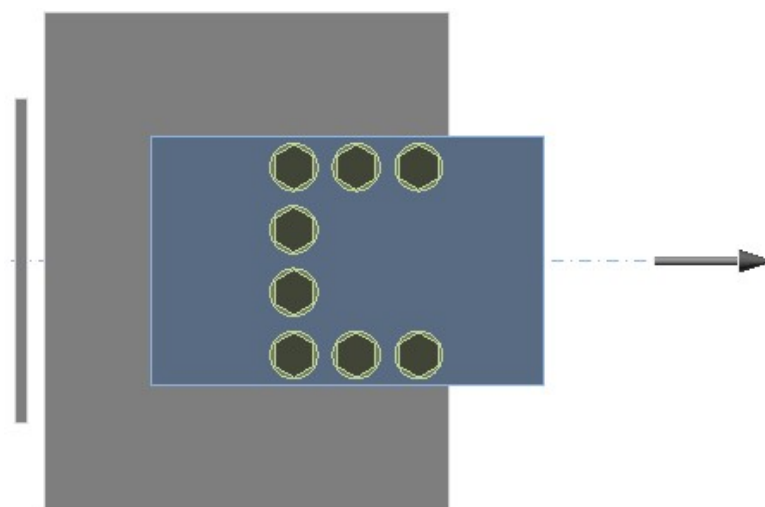


Figure 5.2 - CBFEM model T2

5.1.1 VERIFICATION

According to (Wald et al., 2017), verification is a process where the computational solution is compared with highly accurate analytical or numerical benchmark solution. Unlike validation, experimental data are treated separately in case of verification. The reason for that are unavoidable errors associated with the experimental results.

In this part, CBFEM models are compared with validated ROFEA models from chapter 4 and analytical models obtained from selected codes and scientific papers.

In software, as a default configuration AISC 360-10 is used, material factors equal to 1 and finite elements' size is set to vary from 5 to 10 mm. The ultimate load for CBFEM models is assumed to appear when strain reaches 5%.

Differences between models

In IDEA StatiCa software, the bolts can't be modelled match drilled but only with a gap between the bolt and a plate as it is common in design practice. The bolt holes in IDEA StatiCa for ¾ inches bolts have 20,6 mm in diameter, instead of 19,05 mm as is the case in the experiment / ROFEA. This reduces the shear and tension plane areas and affects the block shear resistance of a joint negatively. Because of this, it is required to consider a contribution to resistance, which is equal to the difference between each areas' resistances:

$$F_{0,05} = F_{0,05,IDEA} + (A_{nt,TEST} - A_{nt,CBFEM}) \cdot F_u + 0,6 \cdot (A_{nv,TEST} - A_{nv,CBFEM}) \cdot F_u \quad (17)$$

or

$$F_{0,05} = F_{0,05,IDEA} + (A_{nt,TEST} - A_{nt,CBFEM}) \cdot F_u \quad (18)$$

where

$F_{0,05}$ is force causing 5% strain plus the contribution to resistance [N]

$F_{0,05,IDEA}$ is force causing 5% strain, value from IDEA StatiCa [N]

$A_{nt,TEST}$ is net tension area corresponding to physical test and ROFEA [mm²]

$A_{nt,IDEA}$ is decreased net shear area as considered in IDEA StatiCa [mm²]

$A_{nv,TEST}$ is net shear area corresponding to physical test and ROFEA [mm²]

$A_{nv,IDEA}$ is decreased net shear area as considered in IDEA StatiCa [mm²]

F_u is ultimate tensile strength [MPa]

F_y is yield strength [MPa]

The differences are calculated according to AISC 360-10, which is also the theoretical background used in the software.

The equations are chosen with respect to governing failure mode.

For T1, gross shear plane yielding followed by tension rupture:

$$F_{0,05} = 504000 + (211 - 200,8) \cdot 450 = 508590 \text{ N (1\% difference)}$$

For T2, shear plane rupture followed by net tension rupture:

$$\begin{aligned} F_{0,05} &= 533000 + (634 - 603,3) \cdot 450 + 0,6 \cdot (1049 - 997,9) \cdot 450 \\ &= 560625 \text{ N (5\% difference)} \end{aligned}$$

Stress vs. strain behaviour determination

Since the cross-sectional area of tested specimens changes in a plastic region during the test (necking on a tension plane etc.), there are two possible ways how to calculate stress vs. strain behaviour.

It can be calculated either by considering the unchanged cross-sectional area, and therefore the engineering stress would be calculated as:

$$\sigma_{engineering} = \frac{F}{A_0} \quad (19)$$

where F is an acting force [N]

A_0 is an initial cross-sectional area [mm²]

Or the true stress, considering the actual cross-sectional area may be obtained from:

$$\sigma_{true} = \frac{F}{A} \quad (20)$$

where A is an instantaneous cross-sectional area [mm²]

Formulas used for the conversion between true and engineering values are according to ČSN EN 1993-1-5: 2006:

$$\sigma_{true} = \sigma_{engineering} \cdot (1 + \varepsilon_{engineering}) \quad (21)$$

$$\varepsilon_{true} = \ln(1 + \varepsilon_{engineering}) \quad (22)$$

Since ANSYS results include true stress versus true strain behaviour, retrospectively, it can be determined what ε_{true} corresponds to 5% $\varepsilon_{engineering}$. Knowing this, it is then possible to find a displacement causing that strain and a corresponding acting force $F_{0,05}$. This force is used in further CBFEM model verification process.

Figures 5.3 and 5.4 show the dependence of true / engineering stress versus strain.

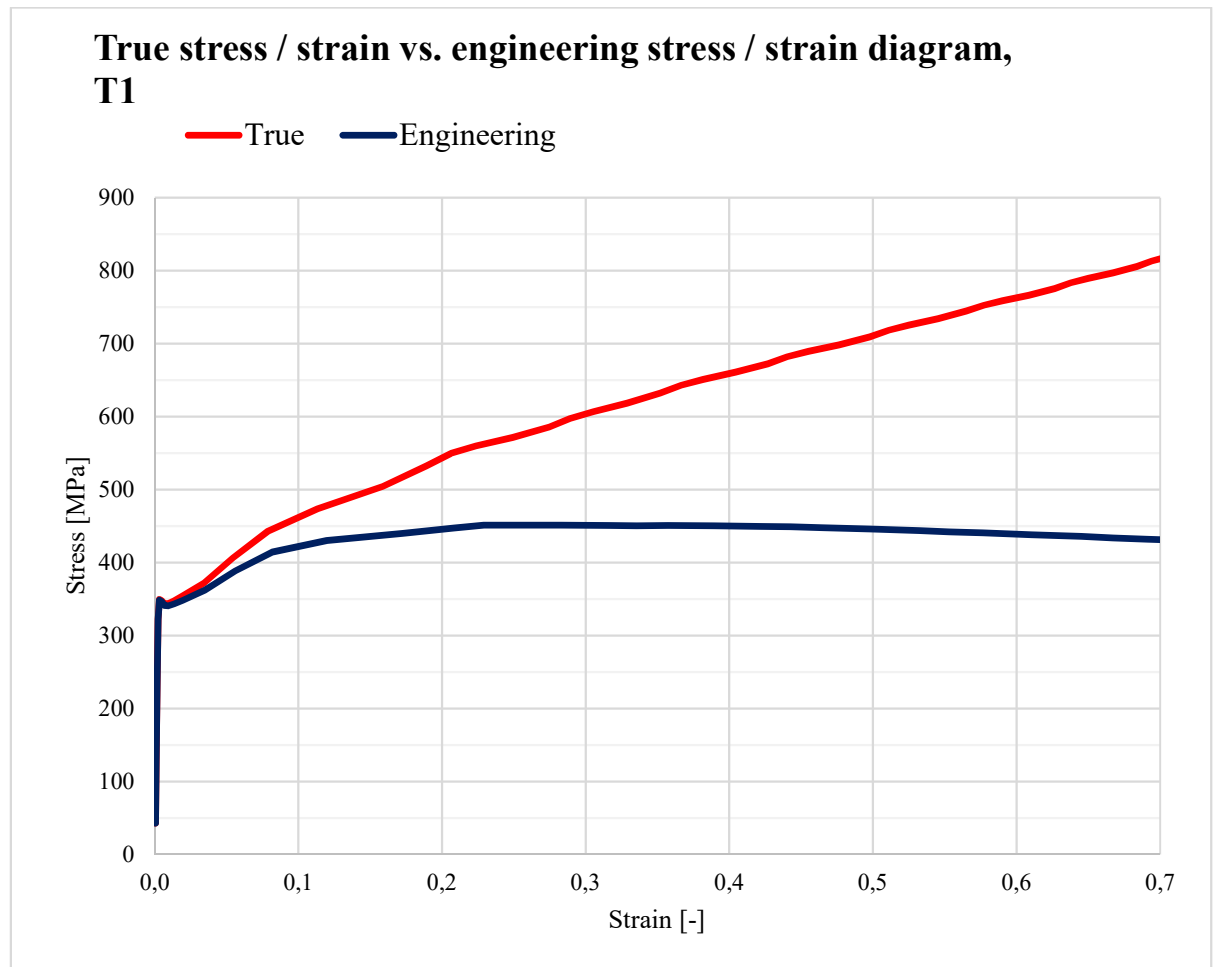


Figure 5.3 - True stress vs. strain and engineering stress vs. strain curves, T1

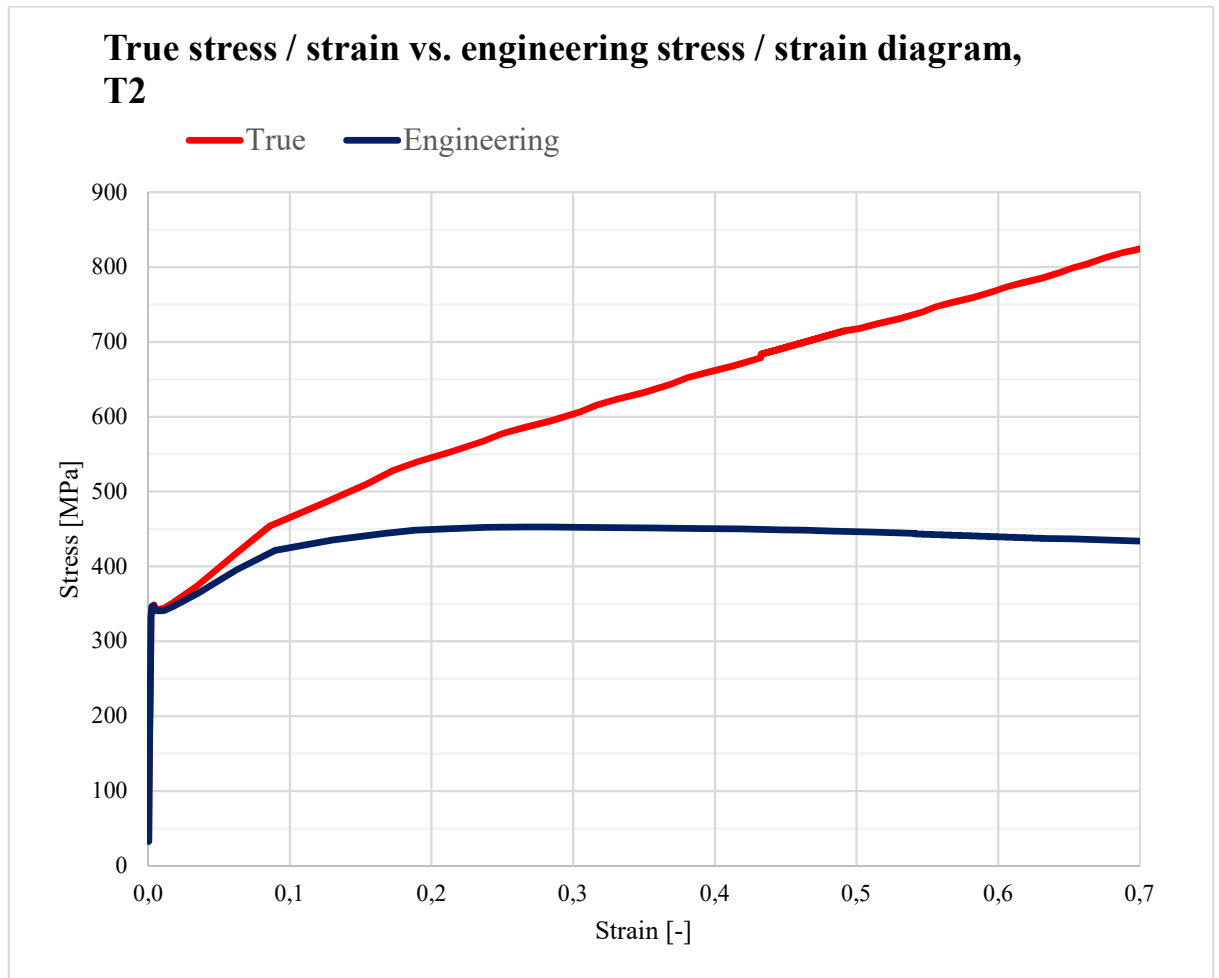
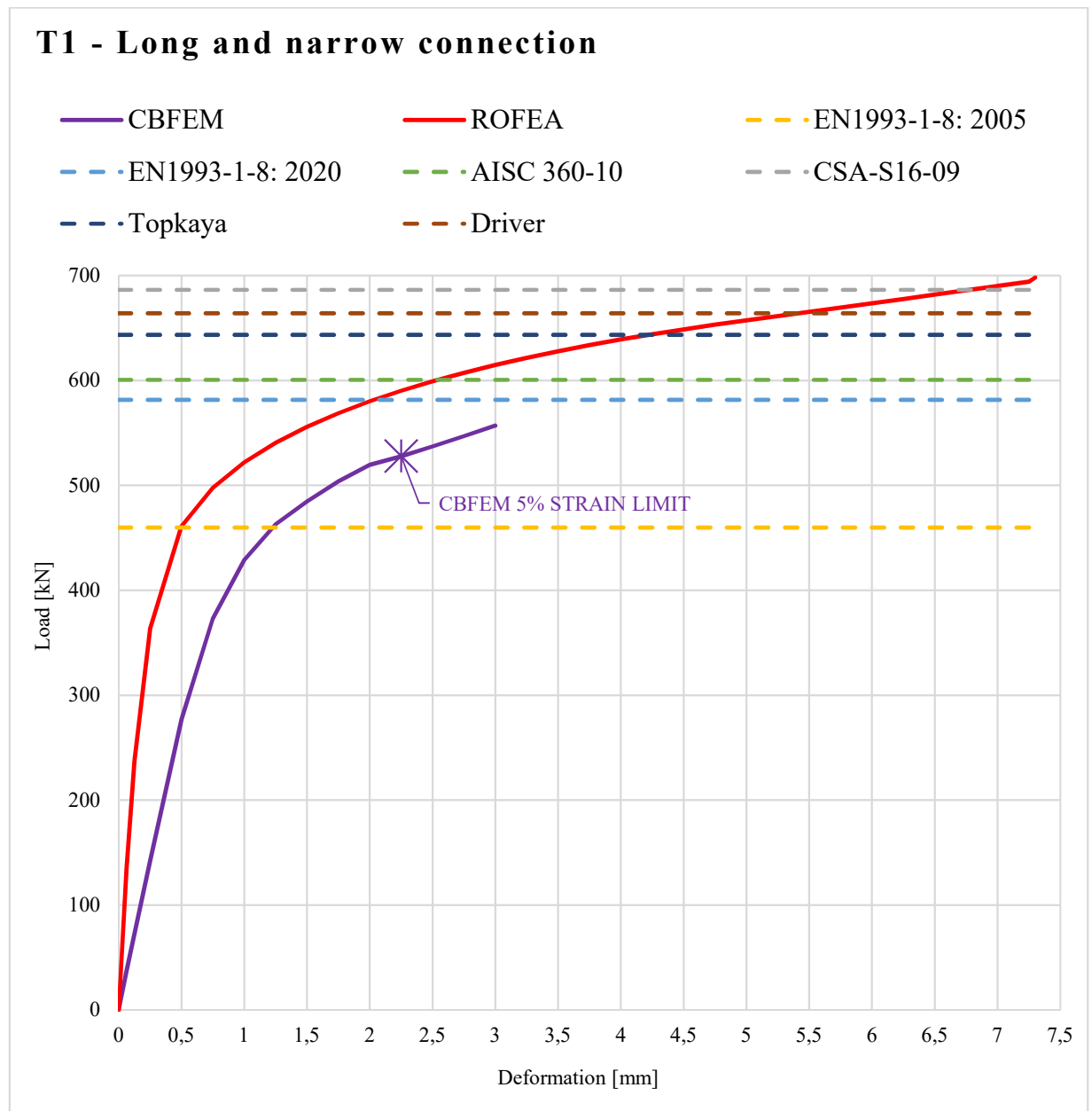


Figure 5.4 - True stress vs. strain and engineering stress vs. strain curves, T2

Verification results**Figure 5.5** - Load versus deformation curves, T1 - verification results

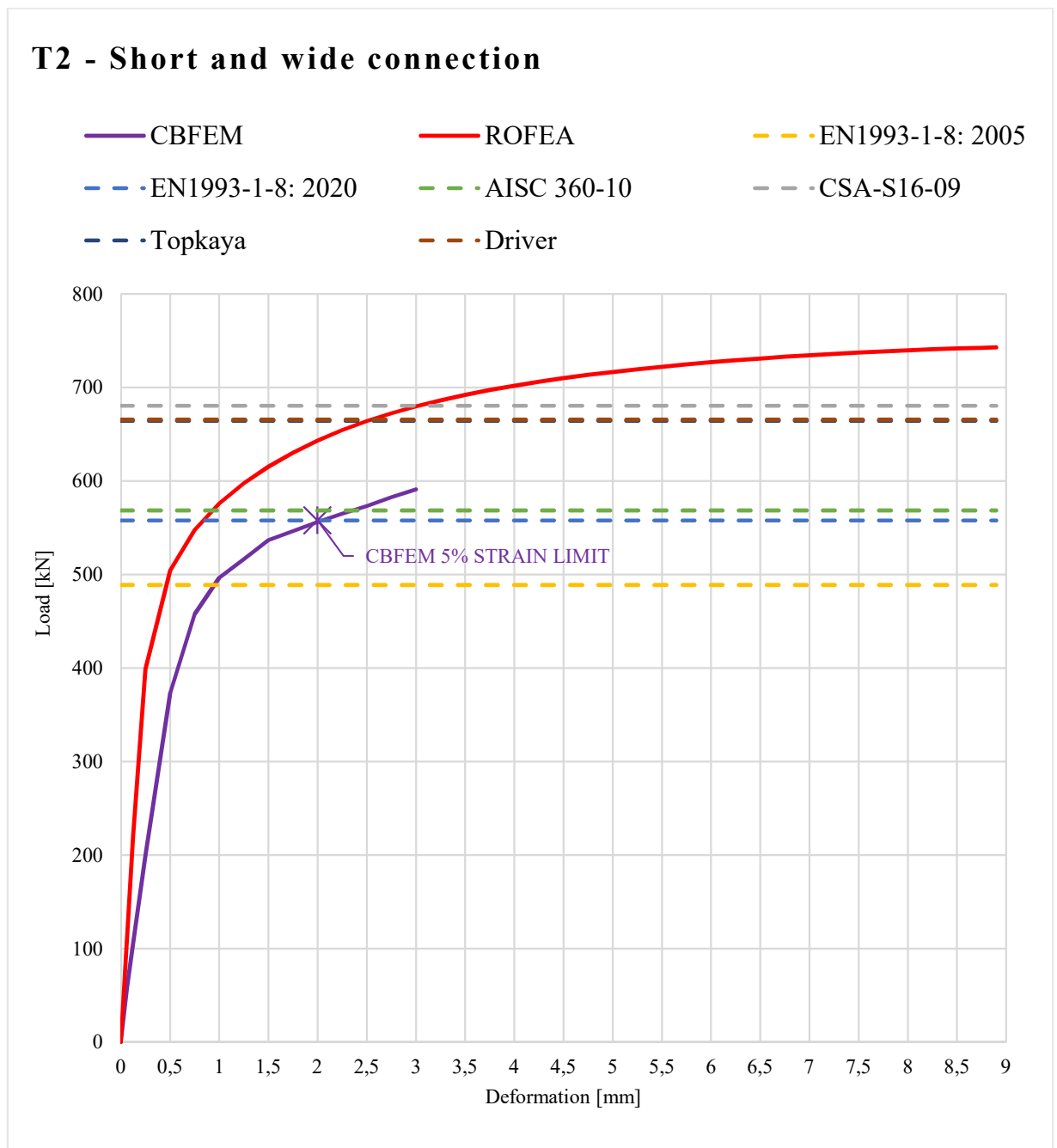


Figure 5.6 – Load versus deformation curves, T2 - verification results

Table 5.1 – Comparison of CBFEM and ROFEA model, T1

T1 specimen	Values			CBFEM vs. ROFEA ratio [-]
Compared parameters	Units	ROFEA	CBFEM	
$N_{j,ini}$	[MN/m]	2153,4	594,3	0,28
F_{peak}	[kN]	698,1	523,0	0,75
F_{2mm}	[kN]	580,1	519,7	0,90
$F_{0,05}$	[kN]	486,3	523,0	1,08
$F_{2/3}$	[kN]	654,5	519,7	0,79

Table 5.2 - Comparison of CBFEM and various analytical models, T1

T1 specimen	Limit load [kN]	CBFEM vs. analytical model ratio [-]
Compared models		
CBFEM	523,0	-
EN1993-1-8:2005	459,8	1,14
EN1993-1-8:2020	581,5	0,90
AISC 360-10	600,6	0,87
CSA-S16-09	686,3	0,76
Topkaya	643,4	0,81
Driver	664,0	0,79

Table 5.3 - Comparison of CBFEM and ROFEA model, T2

T2 specimen	Values			CBFEM vs. ROFEA ratio [-]
Compared parameters	Units	ROFEA	CBFEM	
$N_{j,ini}$	[MN/m]	1773,1	932,8	0,53
F_{peak}	[kN]	742,9	554,4	0,75
F_{2mm}	[kN]	643,3	556,3	0,86
$F_{0,05}$	[kN]	421,0	554,4	1,32
$F_{2/3}$	[kN]	726,5	556,2	0,77

Table 5.4 – Comparison of CBFEM and various analytical models, T2

T2 specimen	Limit load [kN]	CBFEM vs. analytical model ratio [-]
Compared models		
CBFEM	554,4	-
EN1993-1-8:2005	488,8	1,13
EN1993-1-8:2020	557,8	0,99
AISC 360-10	568,5	0,98
CSA-S16-09	680,5	0,81
Topkaya	664,5	0,83
Driver	665,6	0,83

The CBFEM versus analytical model ratio describes how conservative or unconservative the CBFEM model compared to other models is. If the ratio is lower than 1, it means that the CBFEM model is on a side of safety.

From the results above it is apparent, that CBFEM versus analytical model ratios are, except the current valid EN 1993-1-8: 2005, conservative. There is also very high rate of compliance with upcoming EN 1993-1-8: 2020 (90 % and 99 %) and with AISC 360-10 (87 % and 98 %). As it was mentioned before the EN 1993-1-8: 2005 does not take into account two possible modes of block tearing progress and instead of it uses the worst combination.

From the comparison of design-oriented and research-oriented models it is clear that, except the $F_{0,05}$ value, which is more elaborated in following paragraph, all other CBFEM results are on a side of safety. For both CBFEM models, the initial stiffness, $N_{j,ini}$, seems overly conservative when compared to ROFEA model, even though the higher rate of difference is acceptable in case of initial stiffness. This may be caused by the different meshing density of each model, more advanced material description in ROFEA model, see Fig 5.7, component representation of bolts in case of CBFEM model instead of infinitely rigid remote displacement used in ROFEA and some minor deformation of splice plates which are used in CBFEM model. Other CBFEM results are reasonably compliant with the ROFEA results and as it was mentioned, on a side of safety.

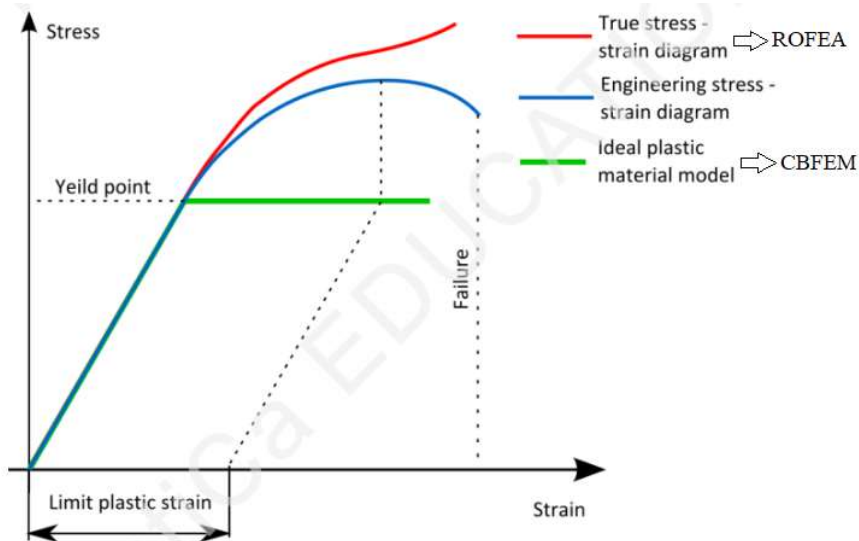


Figure 5.7 – Real tension curve and the ideal elastic-plastic diagram of material, *IDEA StatiCa*

The distinction between $F_{0,05}$ values is probably caused by the fact, that the strain is a local characteristic and it is highly dependent on the mesh element size and type. The difference between mesh density of the research-oriented model and of the design-oriented model is logical but makes the comparison of $F_{0,05}$ problematic. To support this statement, an additional $F_{0,05}$ was obtained from one of the models compared in chapter 4.3.

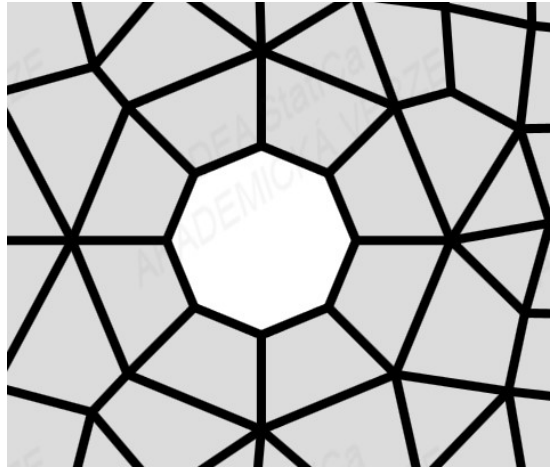


Figure 5.8 - Design-oriented model's mesh – detail of bolthole, $F_{0,05}$, 554,4 kN

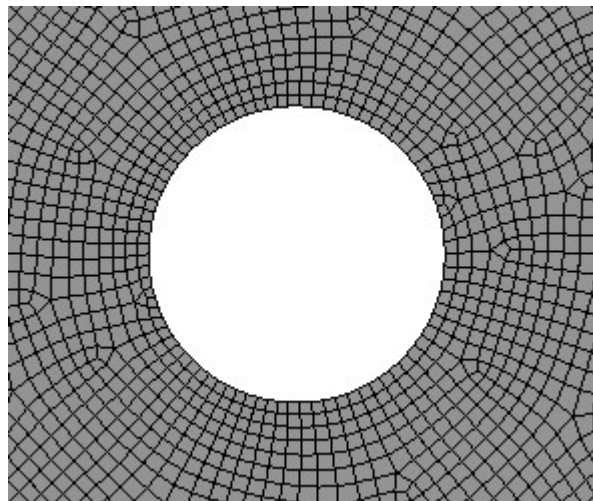


Figure 5.9 – Dense, research-oriented model's mesh 4 – detail of bolthole, $F_{0,05} = 421,0$ kN

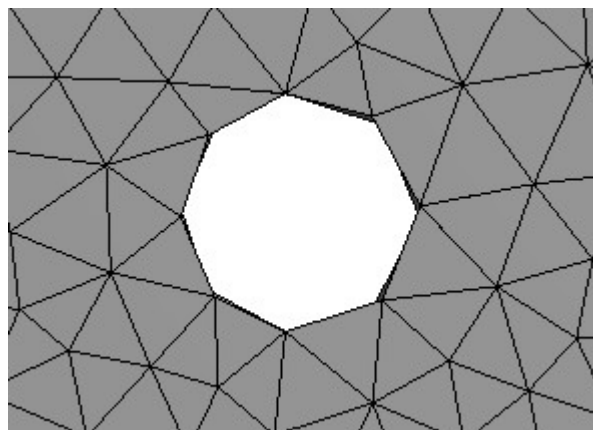


Figure 5.10 – Research-oriented model's mesh 1 – detail of bolthole, $F_{0,05} = 602,0$ kN

As apparent, there are differences not only between research-oriented and design-oriented models, but also between two research-oriented models with different element sizes.

5.1.2 SENSITIVITY STUDY

A sensitivity study (or parametric study) is a technique used for determination how independent input variable values impact dependent output values. It tests how robust the numerical model is.

For the sensitivity study, the CBFEM model T1 is used. Selected variable input parameters are pitch distance and plate thickness. Materials are similar to those mentioned in chapter 2.6.2. The output value subjected to comparison is the ultimate strength of the joint. This value is then compared to the results obtained by different design standards.

The CBFEM model's ultimate resistances are calculated according to AISC 360-10 standard with the LRFD method. The ultimate resistance for CBFEM model is assumed to appear when the strain reaches 5%. The CBFEM results are plotted together with the analytical model results of recent and oncoming codes - EN 1993-1-8: 2005, AISC 360-10, EN 1993-1-8: 2020.

Pitch distance

The first parameter observed is the pitch distance. The study is carried out for 4 different pitch distances:

Pitch distance - p [mm]	56	66	76	86
---------------------------	----	----	----	----

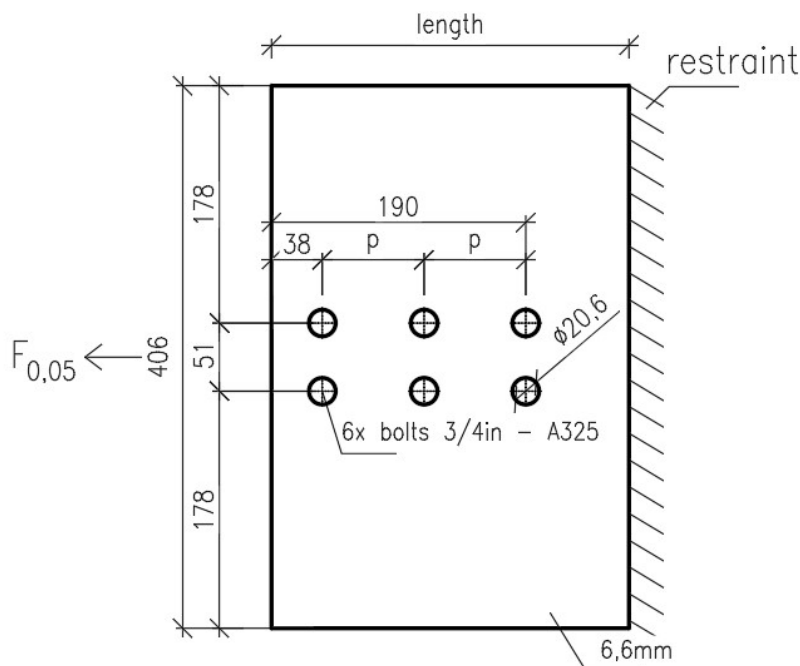


Figure 5.11 - Scheme of the CBFEM model with variable pitch distance

Plate thickness

The second parameter examined is the plate thickness. The study is carried out for 6 different plate thicknesses:

Plate thickness - t [mm]	4,6	5,6	6,6	7,6	8,6	9,6
----------------------------	-----	-----	-----	-----	-----	-----

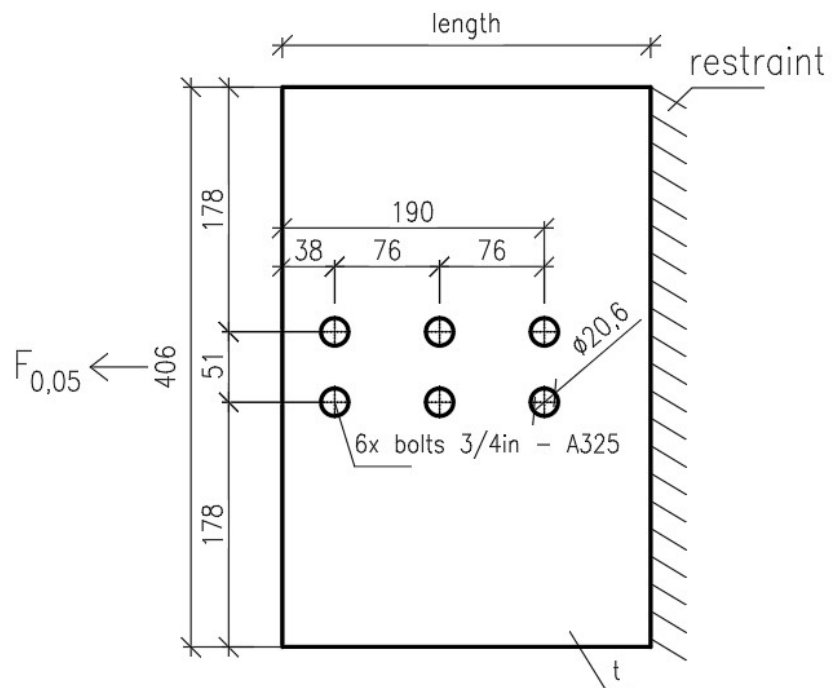


Figure 5.12 - Scheme of the CBFEM model with variable plate thickness

Results

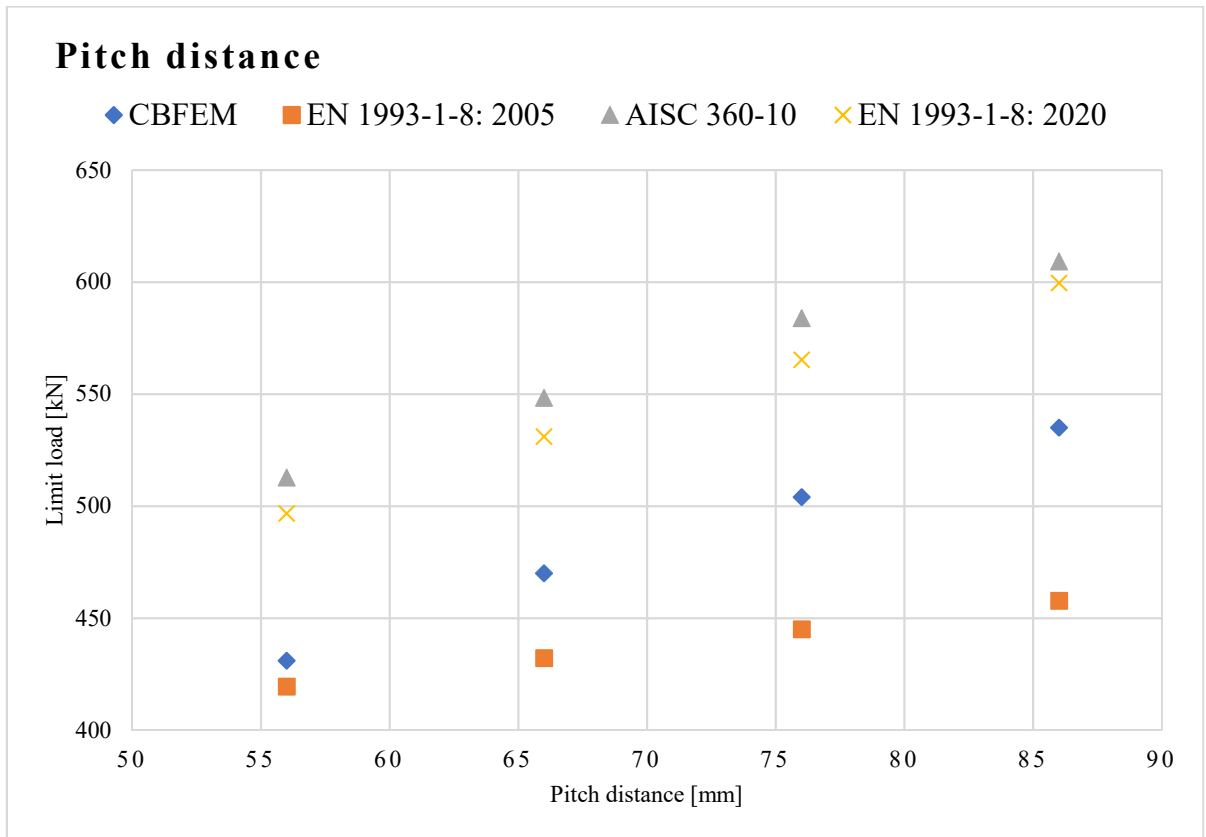


Figure 5.13 - Pitch distance versus limit load diagram

From the diagram, see Fig. 5.13, it can be observed, that, as it was expected, with increasing pitch distance, the resistance grows. The results of CBFEM models are conservative compared to AISC 360-10 and EN 1993-1-8: 2020 standards and unconservative compared to the EN 1993-1-8: 2005. It must be said, that the EN 1993-1-8: 2005 model gives in most cases overly conservative results because of the reasons mentioned in previous chapters and it will be updated in upcoming code's edition.

Also, for CBFEM models, the strain distribution is checked to confirm that the models fail in block shear. Two examples can be seen in Fig. 5.14 and 5.15.

5 % strain:

15 % strain:

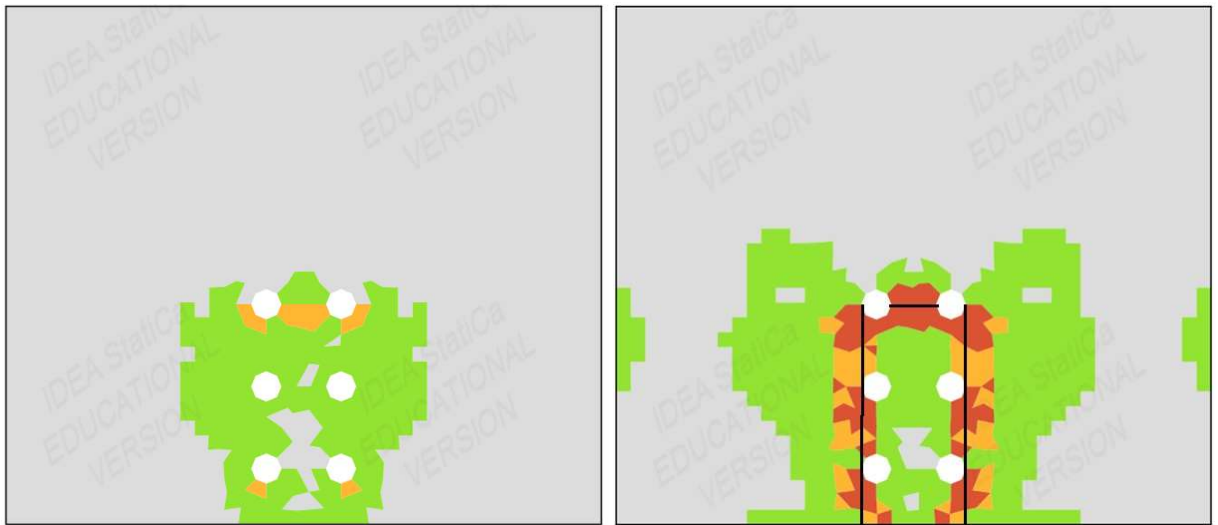


Figure 5.14 - Strain distribution, $p = 56$ mm

5 % strain:

15 % strain:



Figure 5.15 - Strain distribution, $p = 86$ mm

The block shear progression is more apparent in case of the model with smaller pitch distance due to the fact, that with increasing pitch distance the governing failure mode changes into bearing of the plates mode of failure.

Table 5.5 - Pitch distance versus limit load relation

Parameter	Limit load [kN]			
Pitch distance - p [mm]	CBFEM	EN 1993-1-8: 2005	AISC 360-10	EN 1993-1-8: 2020
56	431	419	513	497
66	470	432	548	531
76	504	445	584	565
86	535	458	609	600

The table 5.6 shows CBFEM to specific standard ratio. Default value for CBFEM is set to 1. A ratio above 1 means that the CBFEM model is in that case unconservative, whilst a ratio lower than 1 means that the results of the CBFEM model are compared to the specific standard results conservative.

Table 5.6 – Pitch distance, CBFEM to code results ratio

Parameter	CBFEM to code results ratio [-]			
Pitch distance – p [mm]	CBFEM	EN 1993-1-8: 2005	AISC 360-10	EN 1993-1-8: 2020
56	1	1,03	0,84	0,87
66	1	1,09	0,86	0,89
76	1	1,13	0,86	0,89
86	1	1,17	0,88	0,89

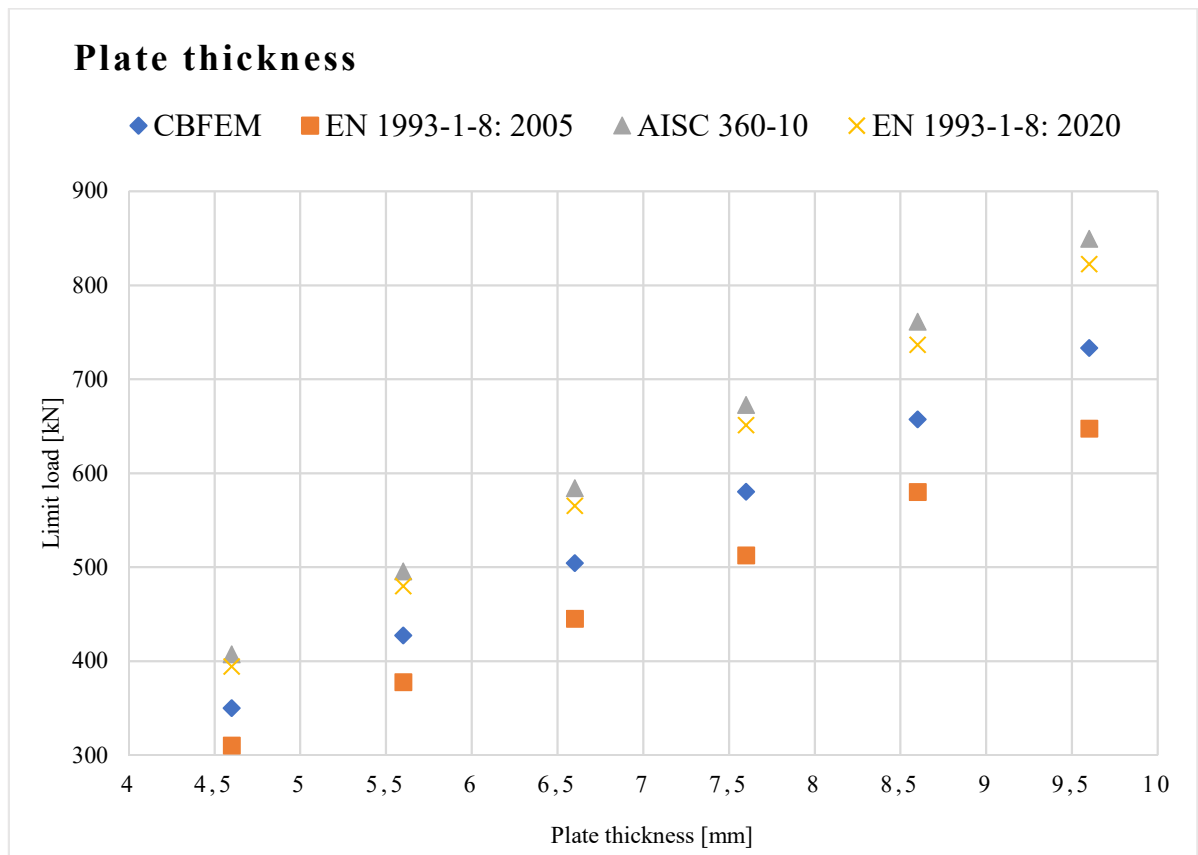
**Figure 5.16 - Plate thickness versus limit load diagram**

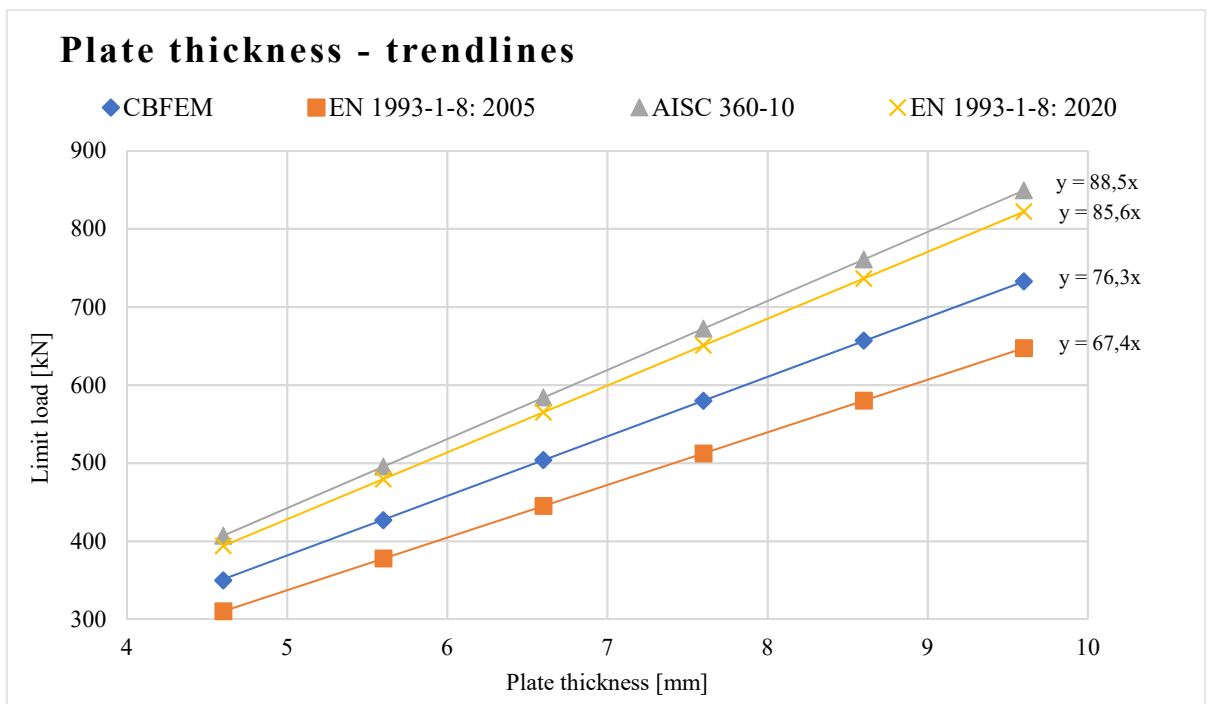
Table 5.7 - Plate thickness versus limit load relation

Parameter	Limit load [kN]			
	CBFEM	EN 1993-1-8: 2005	AISC 360-10	EN 1993-1-8: 2020
4,6	350	310	407	394
5,6	427	378	495	480
6,6	504	445	584	565
7,6	580	512	672	651
8,6	657	580	761	737
9,6	733	647	849	822

From the diagram it is apparent that with increasing plate thickness, the ultimate resistances of models grow, which is in agreement with an assumption. The assumption also was that the growth will be linear, as the models are all linearly dependent on the plate thickness parameter. This assumption has also proved to be true.

Likewise, as with pitch distance parameter, the results of CBFEM are conservative compared to AISC 360-10 and EN 1993-1-8: 2020 standards and unconservative in case of EN 1993-1-8: 2005.

In the graph in Figure 5.17 there is an interleaved linear function through the results that describes the dependence of each model on the plate thickness. The description for each function has also been added, where the slope represents how fast does the ultimate resistance grow in relation to the increment of plate thickness.

**Figure 5.17 - Plate thickness – trendlines**

5.2 ECCENTRIC CONNECTION

The eccentric connection in this work is represented by the tee profile connected through its leg to two symmetric splice plates.

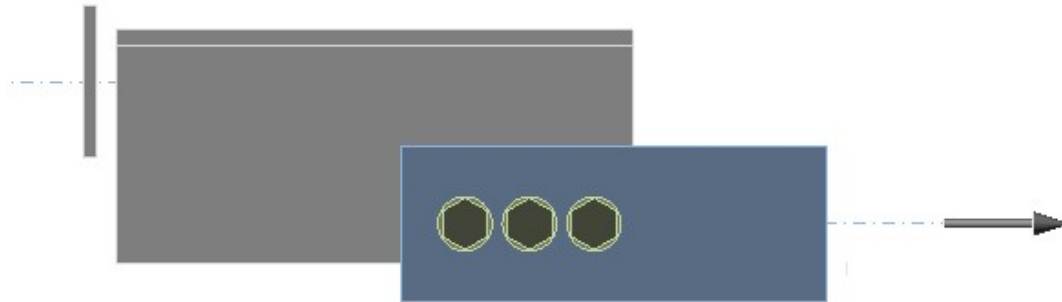


Figure 5.18 – CBFEM model, eccentric connection

5.2.1 GEOMETRY

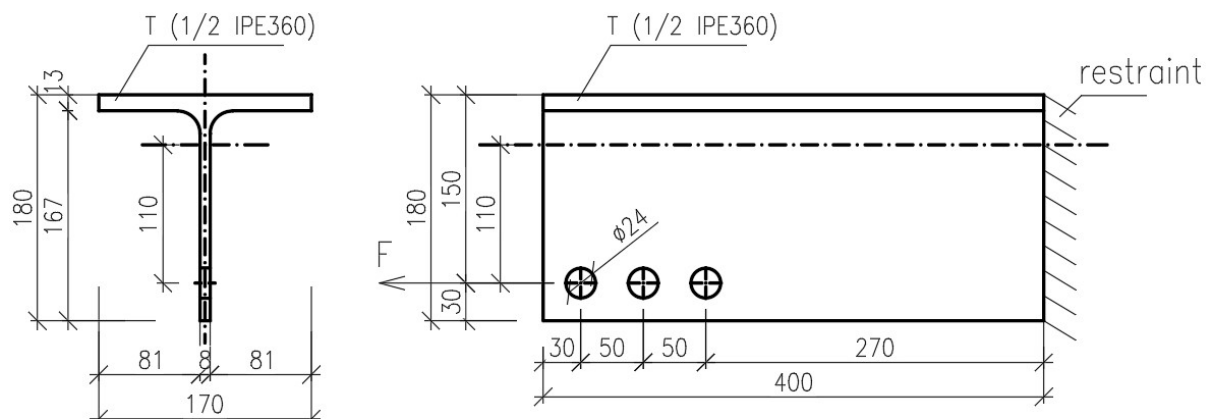


Figure 5.19 - Eccentric model's geometry

5.2.2 MATERIALS

As for materials, steel S235 and bolts M22 - 10.9 are used. Material design factors are equal to 1.

	F_y [MPa]	F_u [MPa]	E [MPa]	ν [-]
Steel S235	235	360	210000	0,3
Bolts 10.9	900	1000	210000	0,3

5.2.3 VERIFICATION

In this part, CBFEM model is compared to analytical models.

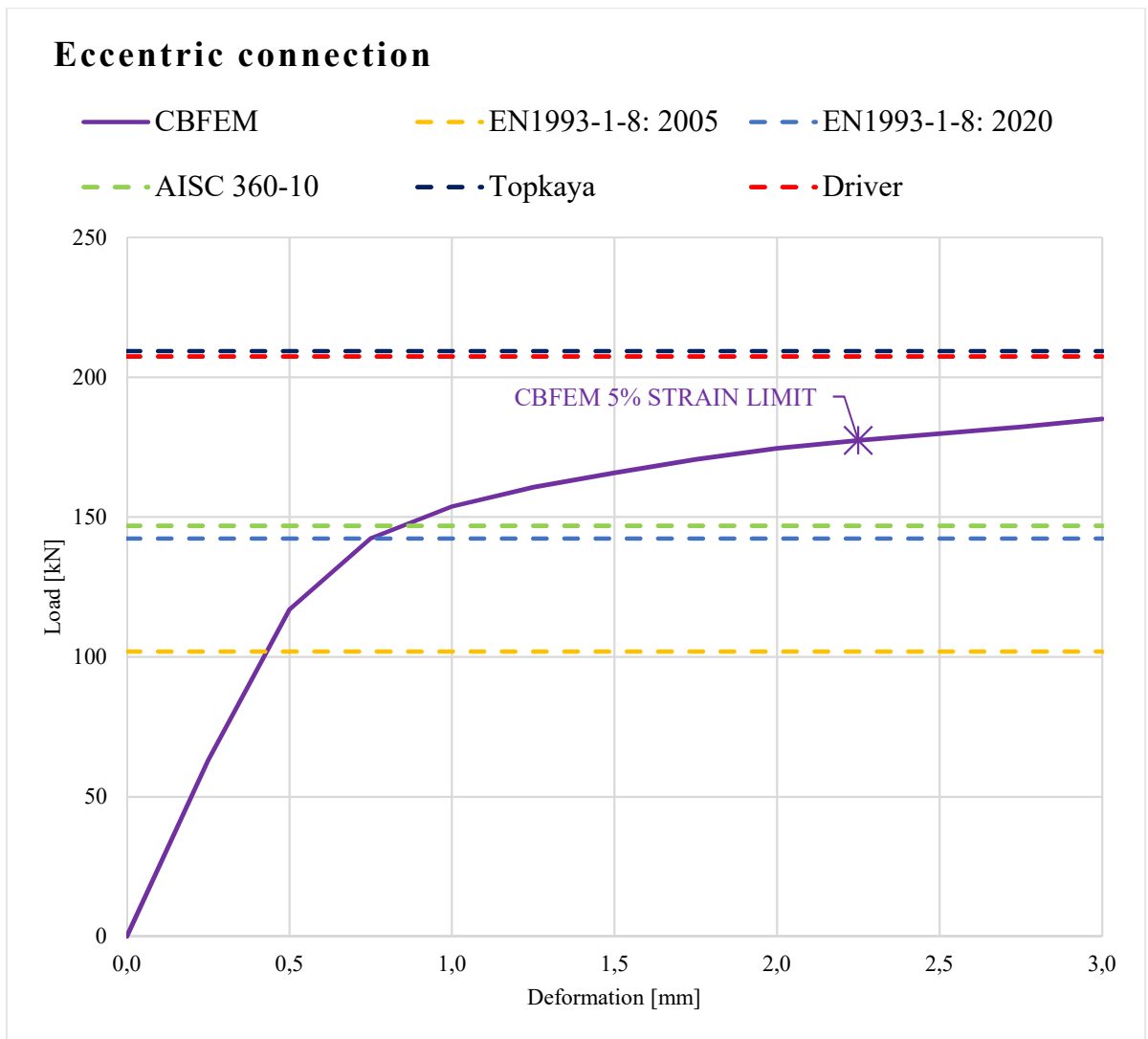


Figure 5.20 - Load versus deformation curves, eccentric connection

Table 5.8 – Comparison of CBFEM and various analytical models, T2

Eccentric connection	Limit load [kN]	CBFEM vs. analytical model ratio [-]
Compared models		
CBFEM	176,0	-
EN 1993-1-8: 2005	101,9	1,73
EN 1993-1-8: 2020	142,3	1,24
AISC 360-10	146,9	1,20
Topkaya	209,4	0,84
Driver	207,4	0,85

As apparent from the results, CBFEM model is unconservative compared to codes' results and conservative compared to Topkaya's and Driver's analytical models. It is due to the fact, that while Driver and Topkaya say, that the effect of in plane eccentricity is not crucial for the total resistance (up to 10 % reduction), in codes, the reduction is significantly higher. CBFEM results lay in between these two design approaches. In contrast to analytical models where the constant reduction of resistance is used, CBFEM models employ finite element analysis for the calculations which may be advantageous in covering the actual size of the eccentricity.

5.2.4 SENSITIVITY STUDY

As a variable input value, the size of the eccentricity is selected. The output value that is subjected to a comparison is the ultimate resistance of the joint and it is compared to the results obtained by different analytical models.

The code configuration used in software is EN 1993-1-8: 2005, material factors equal to 1. As an ultimate load the force causing the 5 % strain is taken. The CBFEM results are plotted together with the analytical models' results of recent and oncoming codes - EN 1993-1-8: 2005, AISC 360-10, EN 1993-1-8: 2020.

The study is carried out for 4 eccentricity sizes:

Size of eccentricity - e [mm]	80	90	100	110
---------------------------------	----	----	-----	-----

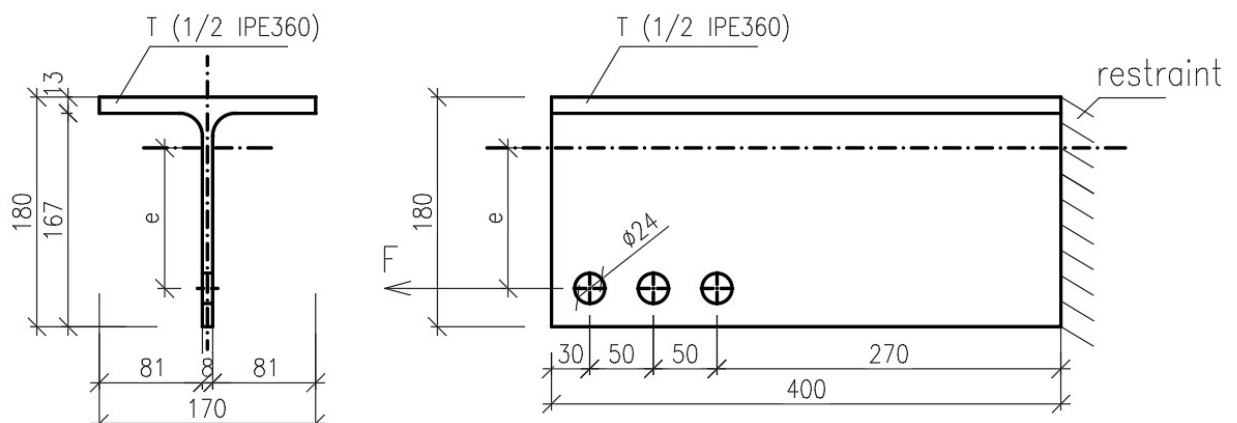


Figure 5.21 - Scheme of the CBFEM model with variable eccentricity

Results

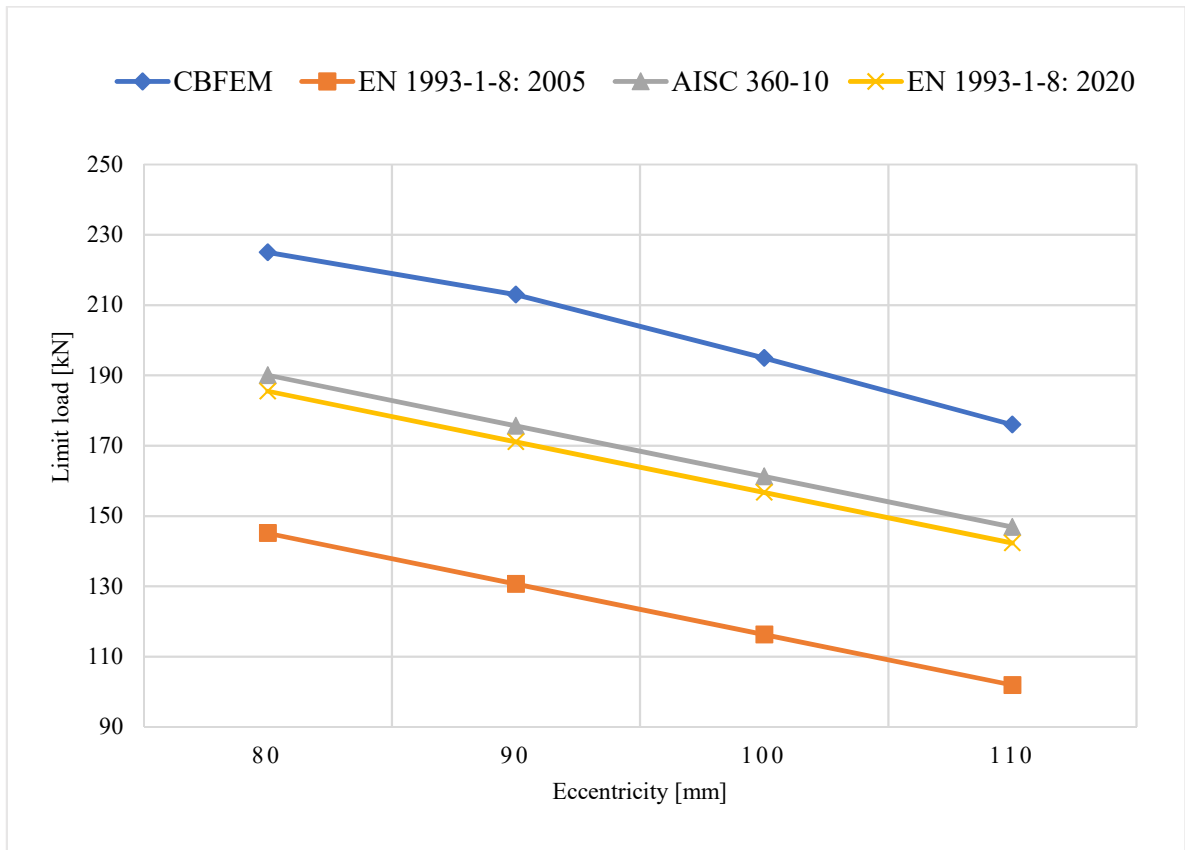


Figure 5.22 – Eccentricity versus limit load plot

Table 5.9 - Eccentricity versus limit load relation

Parameter	Limit load [kN]			
Eccentricity – e [mm]	CBFEM	EN 1993-1-8: 2005	AISC 360-10	EN 1993-1-8: 2020
80	225	145	190	186
90	213	131	176	171
100	195	116	161	157
110	176	102	147	142

Table 5.10 - Eccentricity, CBFEM to code results ratio

Parameter	CBFEM to code results ratio [-]			
Eccentricity – e [mm]	CBFEM	EN 1993-1-8: 2005	AISC 360-10	EN 1993-1-8: 2020
80	1	1,55	1,18	1,21
90	1	1,63	1,21	1,24
100	1	1,68	1,21	1,24
110	1	1,73	1,20	1,24

From the study results it is obvious, that all models' resistances increase with decreasing eccentricity, which fulfils the expectation. The CBFEM results are unconservative compared to the selected codes' results, but it must be said, that the analytical models don't take into account

the actual size of eccentricity, but they use the constant 50 % reduction of the tension plane capacity, which may be in some cases overly conservative. As it was stated in chapter 5.2.3, Driver and Topkaya suggest smaller reduction of resistance and, furthermore, (Jönsson, 2014) suggests reconsidering the analytical model and he proposes introduction of interaction formulas for design against eccentric block shear failure. It may be also observed, that while the analytical models' resistances have linear relationships, the CBFEM model resistance's decrease seems to be more progressive with an increasing eccentricity. It may be caused by the previously mentioned fact that CBFEM considers more parameters because of the employment of finite element analysis, whereas analytical models in general use a constant reduction.

6 BENCHMARK CASE

According to (Wald et al., 2017), a benchmark case is a study that refers to computer simulations. It should be represented by a relatively simple example, which is easy to understand. Simplicity and comprehensibility, in this case, hold a more important value than the actual practical meaning. The benchmark case calculations should be easy to follow, and therefore all the material properties, boundary and load conditions must be well described.

6.1 BENCHMARK CASE SPECIFICATION

As a benchmark case example, a tension bracing member connected to a gusset plate is selected. The joint consists of a pair of UPE 200 profiles connected through their webs to an 8 mm thick gusset plate. The dimensions and geometry are shown in Figure 6.1. The calculations are carried with the aid of the IDEA StatiCa, version 9 software, which uses CBFEM as a computational method. The results are then verified with analytical models from current valid European standard for steel structures joints - EN 1993-1-8: 2005 and oncoming EN 1993-1-8: 2020. The model is loaded with the axial force F_{Ed} and for the further comparison the force causing 5% strain is used.

6.1.1 GEOMETRY

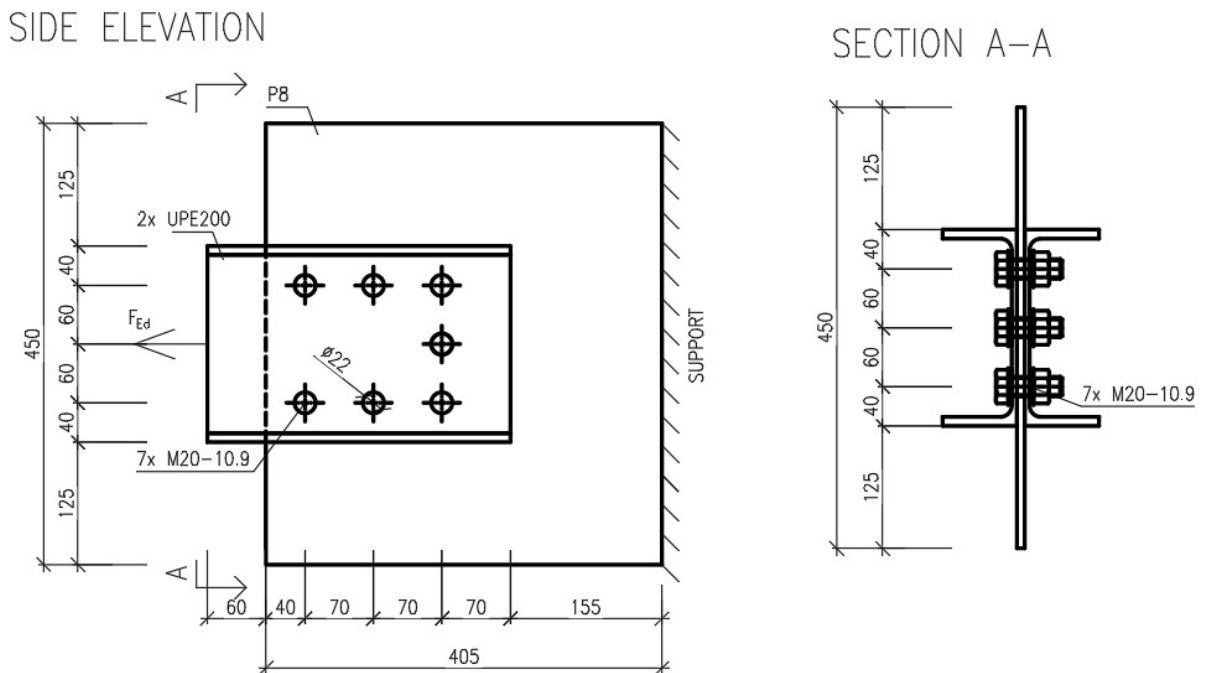


Figure 6.1 - Benchmark example's geometry

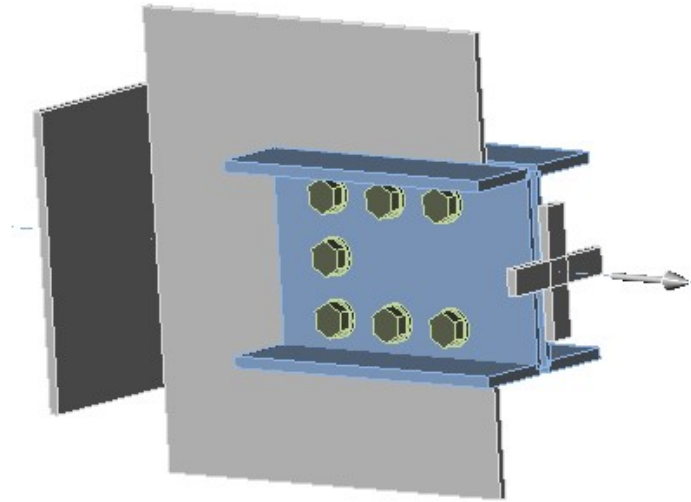


Figure 6.2 – Model of connection, IDEA StatiCa

6.1.2 MATERIALS

As for materials, steel S235 and bolts M20 – 10.9 are used. Material design factors γ_{M0} and γ_{M2} apply.

	F_y [MPa]	F_u [MPa]	E [MPa]	ν [-]
Steel S235	235	360	210000	0,3
Bolts 10.9	900	1000	210000	0,3

6.2 ANALYTICAL MODELS

Since the force acts in the centre of the gravity of the joint, and the bolt configuration is symmetric analytical models for concentric load are used:

6.2.1 EN 1993-1-8: 2005

$$V_{eff,1,Rd} = \frac{f_u A_{nt}}{\gamma_{M2}} + \left(\frac{f_y A_{nv}}{\sqrt{3} \gamma_{M0}} \right)$$

$$f_u = 360 \text{ MPa}$$

$$\gamma_{M2} = 1,25$$

$$f_y = 235 \text{ MPa}$$

$$\gamma_{M0} = 1$$

$$A_{nt} = 608 \text{ mm}^2$$

$$A_{nv} = 2000 \text{ mm}^2$$

$$V_{eff,1,Rd} = \mathbf{446,5 \text{ kN}}$$

6.2.2 EN 1993-1-8: 2020

$$V_{\text{eff},1,\text{Rd}} = \left[A_{\text{nt}} f_u + \min \left(\frac{A_{\text{gv}} f_y}{\sqrt{3}}; \frac{A_{\text{nv}} f_u}{\sqrt{3}} \right) \right] / \gamma_{\text{M2}}$$

$$f_u = 360 \text{ MPa}$$

$$A_{\text{nv}} = 2000 \text{ mm}^2$$

$$f_y = 235 \text{ MPa}$$

$$A_{\text{nt}} = 608 \text{ mm}^2$$

$$\gamma_{\text{M2}} = 1,25$$

$$A_{\text{gv}} = 2880 \text{ mm}^2$$

$$V_{\text{eff},1,\text{Rd}} = \mathbf{487,7 \text{ kN}}$$

6.3 COMPONENT BASED FINITE ELEMENT METHOD

The code background for the calculations carried in IDEA is EN 1993-1-8: 2005, the maximal size of finite elements is set on 10 mm. The values calculated are design values – material coefficients apply. As an ultimate resistance serves the force causing 5 % strain - $F_{\text{Rd},0,05}$. It is then compared to the results of analytical models.

6.3.1 RESULTS

$$F_{\text{Rd},0,05} = 524 \text{ kN}$$

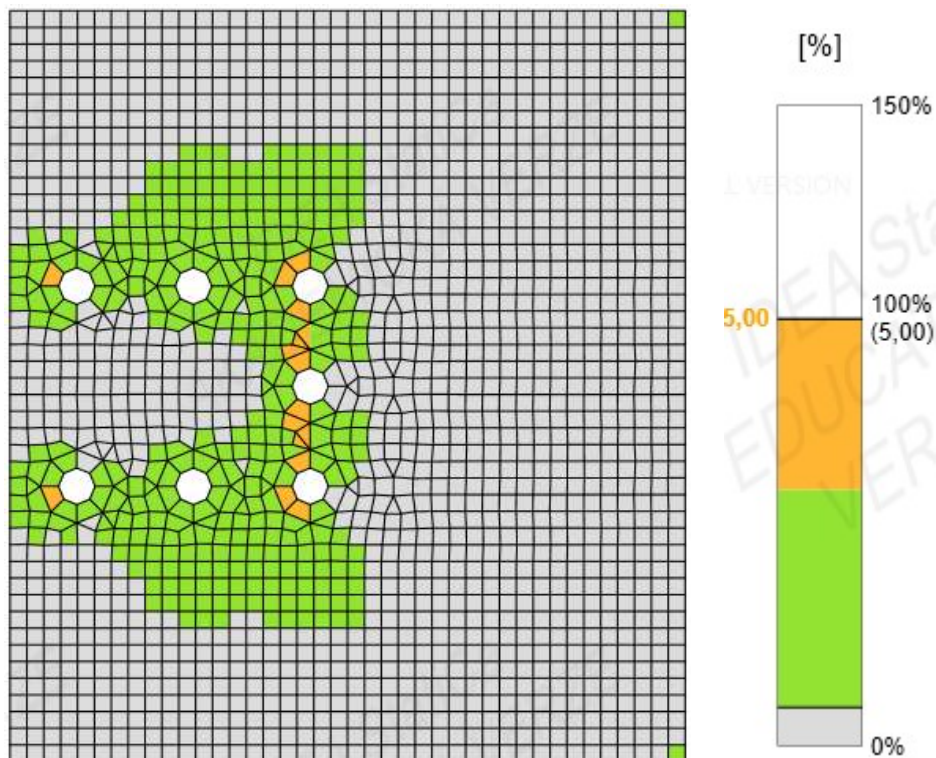


Figure 6.3 – Strain distribution, 5 %

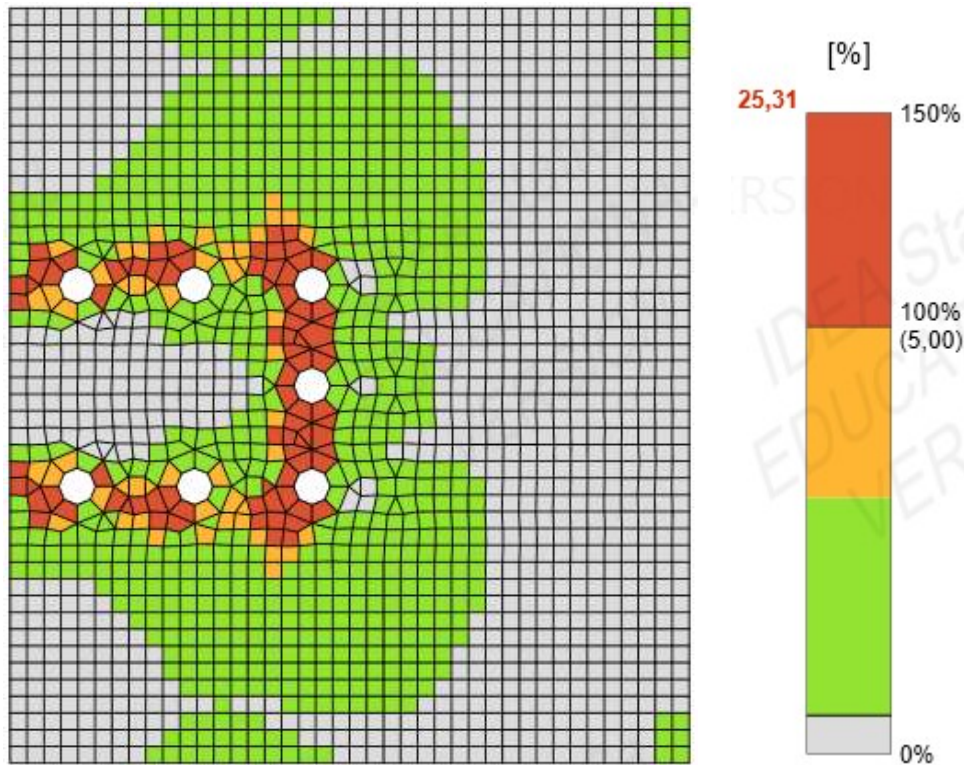


Figure 6.4 - Strain distribution, 25 %

From the strain results, the block shear development may be observed. Figure 6.3 shows that the yielding begins on a tension plane and figure 6.4 shows that the yielding on a gross shear planes follows, which corresponds well to the prediction made by EN 1991-1-8: 2020.

6.4 COMPARISON OF MODELS

The most conservative result of examined joint comes from EN 1993-1-8: 2005 model, then EN 1991-1-8: 2020 follows and the highest resistance can be obtained from CBFEM.

CBFEM to analytical models' ratios:

$$\frac{CBFEM}{EN\ 1993-1-8:2005} = \frac{524}{446,5} = 1,17 \cong 117\% \rightarrow \text{difference } 17\%$$

$$\frac{CBFEM}{EN\ 1993-1-8:2020} = \frac{524}{487,7} = 1,07 \cong 107\% \rightarrow \text{difference } 7\%$$

As was mentioned in previous chapters, the EN 1993-1-8: 2005 model gives overly conservative results in case of block shear failure not only compared to CBFEM but also relative to other analytical models. It may be one of the reasons for the planned revision of the model for block shear failure mode in the next edition of Eurocodes. The model used in

EN 1993-1-8: 2020 is reasonably conformable to the results obtained by the CBFEM method even though CBFEM results are in this case on the unsafe side. The differences may be caused by the fictional limit of 5 % strain for resistance because, in reality, the limit strain can vary for each type joint and failure mode. Also, authors of analytical models tend to create the models that give accurate but rather conservative results. An example can be seen in figure 6.5 where the test versus predicted capacity results based on AISC 1999 are displayed.

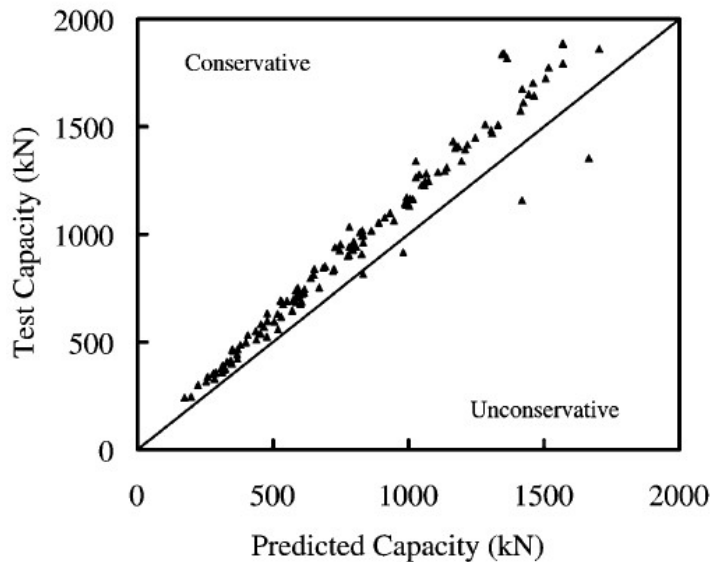


Figure 6.5 - Test capacity vs. predicted capacity based on AISC 1999 (Huns B.B.S., Grondin G., Driver R.G., 2002)

7 CONCLUSION

7.1 VALIDATION

The research-oriented models were validated for two cases of concentric connections and they were created with a use of finite element analysis software – ANSYS Workbench 18.0. Motivation for creating research-oriented models was, that in contrary to analytical models, through advanced models more parameters such as stiffness or load versus deformation curve could be compared. Process of creating included mesh optimisation and simplification of the geometries and loading conditions.

After the advanced numerical solution was obtained chosen parameters were compared and both models had good rate of compliance when compared to experimental data. Therefore, it was possible to use the advanced models in further design-oriented model's verification process.

7.2 VERIFICATION

In this work the design against a block shear failure with the aid of Component based finite element method is verified. In total, including sensitivity studies, 17 CBFEM models were created and compared to either two research-oriented finite element models or 6 different analytical models.

Generally speaking, if the currently valid EN 1993-1-8: 2005 is excluded from the comparison, in case of concentric connections, the CBFEM models have a good rate of compliance with analytical models and, with the exception of one case, they are on a side of safety, see Fig. 7.1.

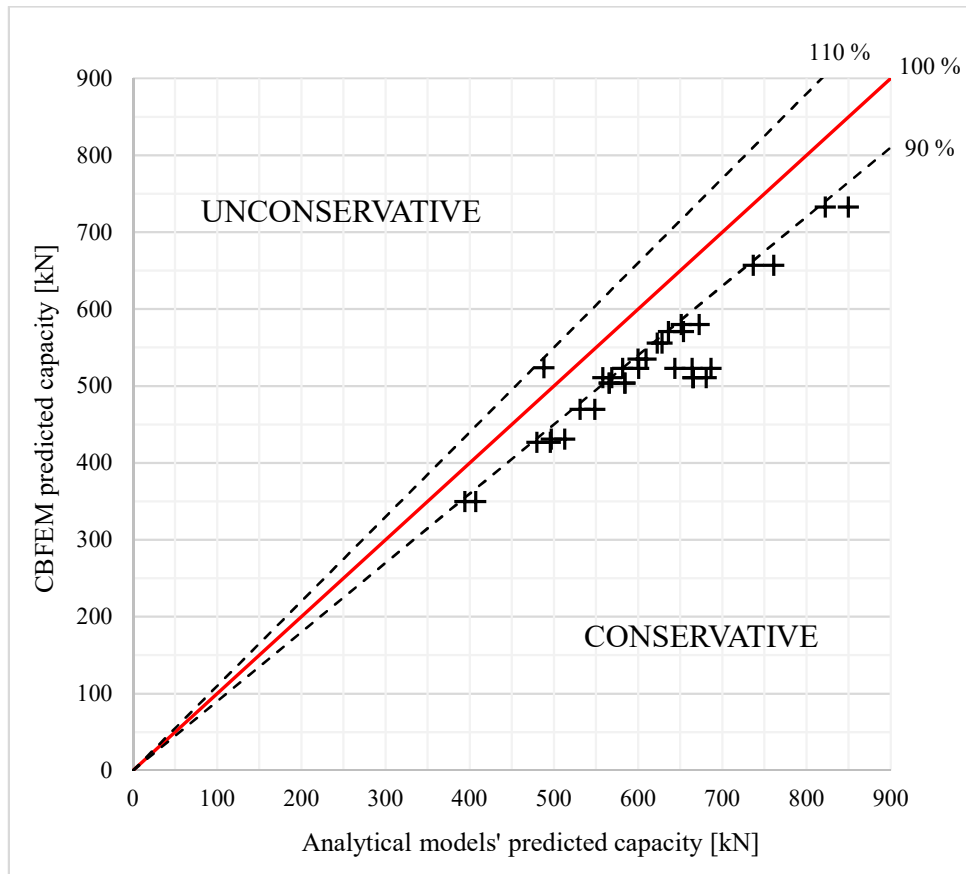


Figure 7.1 - Graphical comparison of predicted capacities, concentric connections

Regarding eccentric connections, the difference between the CBFEM results and analytical models' results is higher, but so is the difference between each analytical model's results depending on the author's approach. Reason for this is the fact that each author gives a different weight to the effect of eccentricity on the connection resistance, see Fig. 7.2.

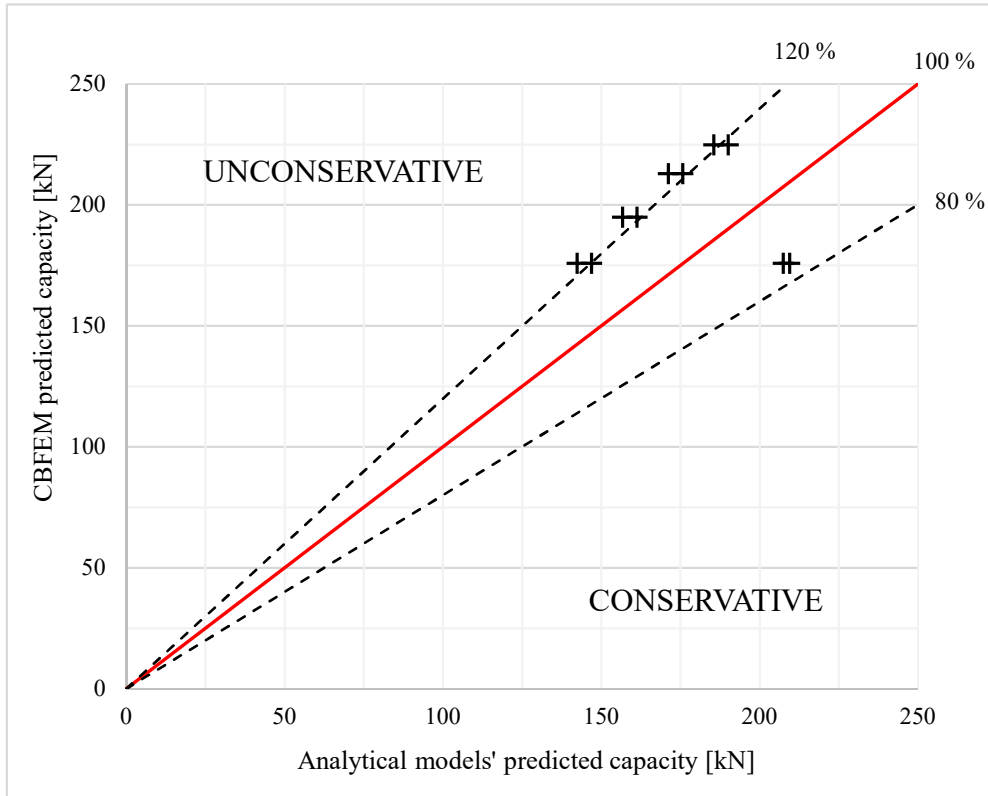


Figure 7.2 - Graphical comparison of predicted capacities, eccentric connections

7.3 FUTURE WORK

As the usage of design oriented finite element models is increasing over the past years, so does the development in this area. On the one hand, the design softwares could make the structural design more efficient and generic, on the other hand, the wrong application, the lack of the subsequent verification and the possibility of using the software without required understanding of the problem may lead to grave mistakes. Therefore, the users of advanced design tools always need to verify the results, meshing and the correct form of application. The next generation of benchmark cases of design against various structural problems should be integrated into the design softwares so the user can easily follow them in the design process.

Concerning the EN 1993-1-8: 2020 oncoming analytical model, it is believed that it corresponds to the block shear failure mode better than the current conservative EN 1993-1-8: 2005. However, in EN 1993-1-8: 2020, the effect of eccentricity is still only considered through a constant reduction of the tension plane resistance, independent of the actual size of eccentricity. Even though the block shear failure mode is typically not the governing mode of failure for the connections with large eccentricity, the actual size of eccentricity should be taken into account in the equation.

REFERENCES

- [1] Topkaya C., A finite element parametric study on block shear failure of steel tension members, *Journal of Constructional Steel Research*, Ankara, 2004
- [2] EN 1993-1-8:2005, *Eurocode 3: Design of steel structures, Part 1.8: Design of joints*. European Committee for Standardisation, Brussels, 2005
- [3] Wald F. et al., *Benchmark cases for advanced design of structural steel connections*, Česká technika – nakladatelství ČVUT, 2017
- [4] EN 1993-1-8:2020, *Eurocode 3: Design of steel structures, Part 1.8: Design of joints*. European Committee for Standardisation, Brussels, final draft, expected 2020
- [5] Robert G. Driver, Gilbert Y. Grondin, Geoffrey L. Kulak, *Unified block shear equation for achieving consistent reliability*, Department of Civil and Environmental Engineering, University of Alberta, 2005
- [6] ČSN EN 1993-1-1:2006, *Eurokód 3: Navrhování ocelových konstrukcí - Část 1.1: Obecná pravidla pro pozemní stavby*. Český normalizační institut, Praha, 2006
- [7] ČSN EN 1993-1-5:2006, *Eurokód 3: Navrhování ocelových konstrukcí - Část 1.5: Boulení stěn*. Český normalizační institut, Praha, 2006
- [8] Kulak G. L., Grondin G. Y., *Block Shear Failure in Steel Members - A Review of Design Practice*. Department of Civil and Environmental Engineering, University of Alberta, 2005
- [9] Šabatka L., Wald F., Kabeláč J., Gödrich L., Navrátil J., *Component based finite element model of structural connections*. IDEA RS s.r.o., 2014
- [10] Radu D., Steel Joints - Component Method Application, *Bulletin of the Transylvania*, University of Braşov, 2012
- [11] Logan D.L., *A first course in finite element method*, United States of America, 2010
- [12] Thornton W., Lini C., *The Whitmore Section*. Modern Steel Construction, 2011
- [13] AISC 360-10, *An American National Standard – Specification for Structural Steel Buildings*, American Institute of Steel Construction, Chicago, 2010

- [14] Bern M., Plassmann P., *Handbook of Computational Geometry*, Elsevier Science B.V., Amsterdam, 2000
- [15] Huns B. B. S., Grondin G. Y., Driver R. G., *Block Shear Behaviour of Bolted Gusset Plates*, Department of Civil and Environmental Engineering, University of Alberta, 2002
- [16] Cai Q., Driver R. G., *End Tear-Out Failures of Bolted Tension Members*, Department of Civil and Environmental Engineering, University of Alberta, 2008
- [17] Jönsson J., *Block Failure in Connections Including Effects of Eccentric Loads*, Technical University of Denmark (DTU), Department of Civil Engineering, 2014
- [18] Whitmore R. E., Experimental Investigation of Stresses in Gusset Plates, *Bulletin No. 16*, Engineering Experiment Station, University of Tennessee, 1952
- [19] The L. H., Drew D. A., Clements D. D. A., *Mechanisms of Block Shear Failure of Bolted Connections*, Missouri University of Science and Technology, 2012

LIST OF TABLES

Table 4.1 – Results of validation, T1	- 34 -
Table 4.2 – Results of validation, T2	- 34 -
Table 5.1 – Comparison of CBFEM and ROFEA model, T1	- 43 -
Table 5.2 - Comparison of CBFEM and various analytical models, T1	- 43 -
Table 5.3 - Comparison of CBFEM and ROFEA model, T2.....	- 43 -
Table 5.4 – Comparison of CBFEM and various analytical models, T2	- 43 -
Table 5.5 - Pitch distance versus limit load relation	- 50 -
Table 5.6 – Pitch distance, CBFEM to code results ratio	- 50 -
Table 5.7 - Plate thickness versus limit load relation.....	- 51 -
Table 5.8 – Comparison of CBFEM and various analytical models, T2	- 53 -
Table 5.9 - Eccentricity versus limit load relation	- 55 -
Table 5.10 - Eccentricity, CBFEM to code results ratio	- 55 -

LIST OF FIGURES

Figure 2.1 - Typical block shear failure mechanism (Cunningham T. J., Orbison J. G., Ziemian R. D., 1994)	- 7 -
Figure 2.2 - The Whitmore section (Thornton W. A., Lini C., 2011)	- 8 -
Figure 2.3 - Effect of boundary conditions on effective stress (Topkaya C. A., 2004).....	- 10 -
Figure 2.4 – Failure planes (Teh L. H., Clements D. D. A., 2012).....	- 13 -
Figure 2.5 - Research oriented finite element models (Topkaya C. A., 2004)	- 17 -
Figure 2.6 - Basic three-dimensional element shapes.....	- 19 -
Figure 2.7 - Grid classifications – a) structured grid b) unstructured grid	- 19 -
Figure 2.8 - Illustrative example of interface and graphical results in IDEA StatiCa 9 – software which employs CBFEM.....	- 20 -
Figure 2.9 - Test set-up (Huns B. B. S., Grondin G., Driver R. G., 2002)	- 21 -
Figure 2.10 - Test specimen T1 (Huns B. B. S., Grondin G., Driver R. G., 2002)	- 22 -
Figure 2.11 - Test specimen T2 (Huns B. B. S., Grondin G., Driver R. G., 2002)	- 22 -
Figure 2.12 - Multilinear isotropic hardening, ANSYS interface.....	- 23 -
Figure 4.1 - Simplified geometries used for FEM simulations.....	- 25 -
Figure 4.2 – Initial concept of bolts	- 26 -
Figure 4.3 - Detail of a bolt hole and nodal selection.....	- 26 -
Figure 4.4 - Automatically generated mesh.....	- 27 -
Figure 4.5 - Dense, automatically generated mesh	- 28 -
Figure 4.6 – Hexahedron-dominant mesh.....	- 29 -
Figure 4.7 – Locally dense, hexahedron-dominant mesh	- 30 -
Figure 4.8 – Comparison of results of different mesh types.....	- 30 -
Figure 4.9 - Comparison of standard deviations.....	- 31 -
Figure 4.10 - Load versus deformation plot, ROFEA and experimental curves, T1	- 33 -
Figure 4.11 – Load versus deformation plot, ROFEA and experimental curves, T2	- 33 -
Figure 4.12 – Deformed bolt hole, necking on a tension plane	- 35 -
Figure 5.1 - CBFEM model T1	- 36 -
Figure 5.2 - CBFEM model T2.....	- 36 -
Figure 5.3 - True stress vs. strain and engineering stress vs. strain curves, T1	- 39 -
Figure 5.4 - True stress vs. strain and engineering stress vs. strain curves, T2	- 40 -
Figure 5.5 - Load versus deformation curves, T1 - verification results.....	- 41 -
Figure 5.6 – Load versus deformation curves, T2 - verification results	- 42 -

Figure 5.7 – Real tension curve and the ideal elastic-plastic diagram of material, IDEA StatiCa.....	- 44 -
Figure 5.8 - Design-oriented model's mesh – detail of bolthole, $F_{0,05}$, 554,4 kN	- 45 -
Figure 5.9 – Dense, research-oriented model's mesh 4 – detail of bolthole, $F_{0,05} = 421,0$ kN	- 45 -
Figure 5.10 – Research-oriented model's mesh 1 – detail of bolthole, $F_{0,05} = 602,0$ kN	- 45 -
Figure 5.11 - Scheme of the CBFEM model with variable pitch distance	- 46 -
Figure 5.12 - Scheme of the CBFEM model with variable plate thickness.....	- 47 -
Figure 5.13 - Pitch distance versus limit load diagram.....	- 48 -
Figure 5.14 - Strain distribution, $p = 56$ mm	- 49 -
Figure 5.15 - Strain distribution, $p = 86$ mm	- 49 -
Figure 5.16 - Plate thickness versus limit load diagram	- 50 -
Figure 5.17 - Plate thickness – trendlines	- 51 -
Figure 5.18 – CBFEM model, eccentric connection.....	- 52 -
Figure 5.19 - Eccentric model's geometry	- 52 -
Figure 5.20 - Load versus deformation curves, eccentric connection	- 53 -
Figure 5.21 - Scheme of the CBFEM model with variable eccentricity.....	- 54 -
Figure 5.22 – Eccentricity versus limit load plot.....	- 55 -
Figure 6.1 - Benchmark example's geometry.....	- 57 -
Figure 6.2 – Model of connection, IDEA StatiCa	- 58 -
Figure 6.3 – Strain distribution, 5 %.....	- 59 -
Figure 6.4 - Strain distribution, 25 %	- 60 -
Figure 6.5 - Test capacity vs. predicted capacity based on AISC 1999 (Huns B.B.S., Grondin G., Driver R.G., 2002)	- 61 -
Figure 7.1 - Graphical comparison of predicted capacities, concentric connections.....	- 63 -
Figure 7.2 - Graphical comparison of predicted capacities, eccentric connections.....	- 64 -